Finanziato dall'Unione europea NextGenerationEU

Accident Risk reduCtion of vulnerAble RoaD usErs: an interdisciplinary – multiperspective approach (ARCADE)

Deliverable 2

WP1 - Observational investigations (Method #1)

T1.2: Field data acquisition

T1.3: Analysis

T1.4: Data collection, treatment, reduction, and modeling

Version:	1
Date	9 September 2025
Drafted:	Gagliardi V., Manalo J., Vennarucci A, Checcherini L. (UniRM3); Hassani Barbin A., Tefa L. (poliTO); Bruno G.,(UniPD)
Validate	Francesco Bella (Principal Investigator – UniRM3) Marco Bassani (Resp. research unit PoliTO) Andrea Spoto (Resp. research unit UniPD)
Authors/members RU	RU-UniRM3: Bella F., Calvi A., D'Amico F., Gagliardi V., Manalo J., Vennarucci A, L. Checcherini RU-PoliTO: Bassani M., Tefa L., Lioi A., Hassani Barbin A. RU-UniPD: Bruno G., Spoto, A.
Keywords:	Road Safety, Vulnerable Road Users, Human Factors, Surrogate Safety Measures, Multiperspective, Biopsychology

WP1 - Observational investigations (Method #1)

T1.2: Field data acquisition from dedicated installations at Hazardous Road Locations (HRL) in the cities of Rome, Turin, and Padua.

T1.3: Analysis conducted using proprietary software, codes, and algorithms.

T1.4: Data collection, treatment, reduction, and modeling to obtain Surrogate Safety Measures (SSMs) for the classification of driver-VRU interactions and the identification of the most effective road safety countermeasures.

Contents

1 Introduction

The purpose of this document (Deliverable 2) is to report on the methodological and technical framework deployed for the field investigations. Specifically, this deliverable illustrates how the selected LiDAR-based architecture and the customized data processing pipeline were implemented to derive robust Surrogate Safety Measures (SSMs) from the raw data recorded by the LiDAR sensor.

In particular, this document details the activities conducted under WP1, Observational investigations (Method #1), and specifically addresses the following tasks:

- T1.2: Field data acquisition from dedicated installations at Hazardous Road Locations (HRL) in the cities of Rome, Turin, and Padua.
- T1.3: Analysis conducted using proprietary software, codes, and algorithms.
- T1.4: Data collection, treatment, reduction, and modeling to obtain Surrogate Safety Measures (SSMs) for the classification of driver-VRU interactions and the identification of the most effective road safety countermeasures.

Section 2, Methods, presents the architecture of the LiDAR system utilized, as well as the acquisition and post-processing workflow for field data, aimed at determining the most appropriate surrogate safety measures to describe the criticality of driver-VRU interactions.

Sections 3, 4, and 5 describe the specific field activities carried out by the three Research Units (RUs), providing concise concluding remarks that highlight the critical issues identified at the investigated sites. This analysis is intended to support the definition of effective safety countermeasures, the efficacy of which will be further investigated through studies performed in a simulated environment (Method #2).

Therefore, this document serves as an essential technical bridge between the preliminary site assessments established in Deliverable 1 and the extensive proactive safety evaluations that will guide the design of targeted, context-sensitive urban interventions in the subsequent phases, specifically simulation studies involving vehicle, motorcycle, and pedestrian simulators, of the ARCADE project.

2 Methods

The methodology adopted in this study translates the proactive safety framework introduced in the previous chapter into a concrete operational pipeline. This approach focuses on the quantitative analysis of road user interactions and the assessment of road safety within urban environments, specifically targeting intersections and pedestrian/cyclist crossings.

The core of this methodology involves the deployment of the “Quanergy MQ-8 LiDAR” sensor for field surveys. LiDAR (Light Detection and Ranging) technology represents an innovative and highly reliable solution for traffic monitoring. Unlike traditional video-based systems, which are highly susceptible to varying lighting conditions, glare, and shadows, the LiDAR sensor enables the non-invasive, continuous acquisition of high-resolution three-dimensional spatial data, ensuring consistent data quality regardless of environmental illumination (Bataineh et al., 2023; Zhang et al., 2020; Vennarucci et al., 2025).

The Quanergy MQ-8 sensor is specifically utilized for its advanced capabilities in detecting moving objects, classifying them by road user type (e.g., pedestrians, cyclists, vehicles), and tracking their trajectories over time. The system generates a precise point cloud that allows for the reconstruction of user movements with high fidelity. Crucially, this tracking capability enables the continuous extraction of detailed kinematic profiles for all interacting users. By monitoring the intersection and pedestrian crossing zones, the system provides precise measurements of instantaneous velocity, acceleration, deceleration, and spatial positioning.

By capturing these complex interaction dynamics, which include subtle behavioral adaptations often imperceptible to human observers or standard inductive loops, the system effectively isolates critical "near-miss" events. To objectively quantify the severity of these interactions and evaluate the safety performance of the intersection, the methodology computes specific Surrogate Safety Measures (SSMs) derived directly from the kinematic data.

2.1 Quanergy MQ-8 LiDAR sensor and System Architecture

The primary data source selected for the field investigations is the Quanergy MQ-8 3D LiDAR sensor (fig. 1). The deployment of Light Detection and Ranging (LiDAR) technology represents a strategic choice to overcome the inherent limitations of traditional 2D optical cameras, such as sensitivity to variable lighting conditions, glare, and the lack of native depth perception.

However, the adopted monitoring solution does not consist solely of the physical sensing device. Rather, it is structured as an advanced, integrated hardware–software architecture designed to handle the full pipeline from raw data acquisition to high-level semantic outputs. This comprehensive ecosystem is composed of four main pillars:

- **MQ-8 LiDAR Sensor:** The hardware edge device responsible for emitting laser pulses and capturing the raw three-dimensional point cloud of the surrounding environment.
- **Qortex DTC (Detection, Tracking, Classification):** The core analytical engine. It processes the massive influx of raw data in real time, executing complex algorithms for background subtraction, object detection, multi-target tracking, and semantic classification.
- **Qortex Client:** The dedicated configuration environment used for system management. It handles critical setup tasks including network configuration, the definition of Regions of Interest (ROIs) and exclusion zones, as well as the management of TCP publishing protocols.
- **Q-View:** A specialized validation software providing a graphical interface. It serves as an essential tool for the qualitative inspection of tracking performance and sensor calibration.

Figure 1 - Instrumentation LiDAR Quanergy MQ-8

The Quanergy MQ-8 belongs to a new generation of multi-beam mechanical LiDAR sensors engineered specifically for the demands of smart city infrastructure and intelligent transportation systems (ITS). It operates using Time-of-Flight (ToF) technology across eight vertically arranged laser channels. By calculating the time taken for emitted light pulses to reflect off surfaces and return to the receiver, the sensor generates high-density 3D point clouds.

The device features a 360° horizontal Field of View (FoV) coupled with an approximately 20° vertical FoV, providing comprehensive spatial coverage of wide intersections. With an angular resolution reaching up to 0.13° and an acquisition rate of up to 1.26 million points per second, the MQ-8 ensures an exceptionally detailed spatial reconstruction of the monitored area. A crucial feature for outdoor deployment is its support for multiple returns; this allows the system to filter out "noise" caused by partial hits on rain, fog, or dust, focusing instead on the solid targets behind them.
Measurement accuracy is strictly maintained within a ±3 cm margin at distances up to 50 meters. This high degree of precision, combined with its environmental robustness, makes it particularly suitable for long-term outdoor traffic monitoring where micro-mobility users (e.g., pedestrians, cyclists) must be distinguished from larger vehicles. The sensor outputs this massive volume of data in real time via TCP/IP, enabling seamless, low-latency integration with the Qortex DTC engine and allowing for custom external data acquisition scripts (e.g., Python-based logging algorithms) to interface directly with the data stream.

To ensure optimal data collection during the experimental campaigns, the physical positioning of the sensor was carefully calculated. The LiDAR was mounted on a stabilized, heavy-duty tripod at an elevation of approximately 3.00 meters above the road surface. This specific height was strategically selected to establish an optimal grazing angle: it is high enough to guarantee comprehensive coverage of the entire intersection while significantly limiting the "shadowing" effect and occlusions typically caused by the transit of large vehicles, such as buses or heavy goods vehicles (HGVs).

To support mobile and potentially remote field acquisitions, the hardware framework was engineered for reliability and continuous operation, incorporating:

- **Uninterruptible Power Supply (UPS):** A Pure Sine Wave UPS was integrated into the setup to provide stable, clean electrical power. This safeguards the LiDAR, the network switch, and the control workstation against voltage fluctuations and ensures continuous operation and data integrity during brief power anomalies.
- **High-Speed Connectivity Setup:** System integration relies on a PoE+ (Power over Ethernet Plus) switch. This dual-purpose setup provides both the necessary electrical power to the sensor and high-

bandwidth data transmission over a single standard Ethernet cable, significantly simplifying the wiring complexity of the mobile setup. The LiDAR communicates with the local control PC via a dedicated, closed local TCP/IP network to prevent packet loss and ensure microsecond synchronization.

The complex transformation of unorganized, raw point clouds into structured, actionable trajectory datasets is executed entirely by Qortex DTC (fig. 2). By applying clustering and tracking algorithms, the software converts raw points into discrete objects. It generates comprehensive object-level outputs that include a unique Track ID, semantic classification (categorizing targets as pedestrians, standard vehicles, or cyclists), continuous 3D spatial coordinates, and dynamic vectors such as velocity and acceleration components.

Prior to recording the data for downstream analytical processing, Q-View was actively employed during the deployment phase as a strict validation interface. Operators utilized Q-View to visually superimpose the digital tracking outputs over the known physical road geometry. This critical calibration step verified the spatial alignment of the coordinate system and ensured the overarching reliability and accuracy of the data acquisition process in the real-world environment.

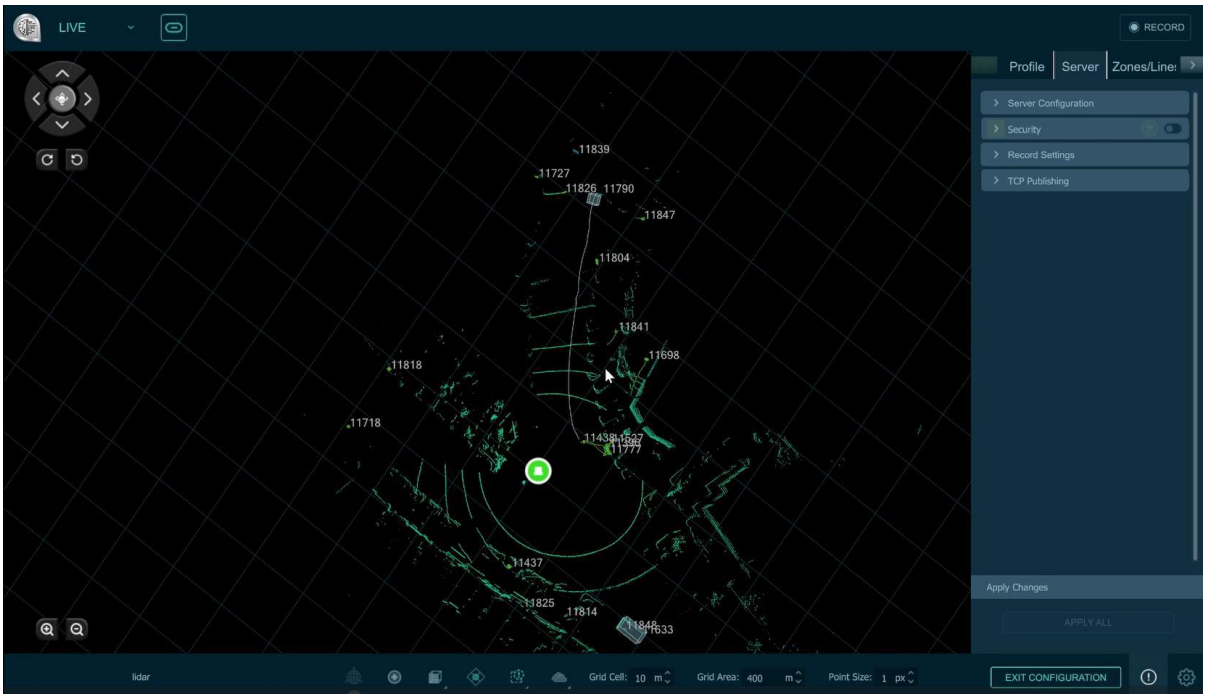

Figure 2 - Qortex DTC software screen

2.2 Data acquisition and processing workflow

2.2.1 UniRomaTre approach

The transition from real-time sensor perception to offline safety analysis is managed through a customized computational workflow developed in **Python**. This middleware bridges the gap between the raw sensor output and the analytical requirements for safety evaluation.

The object list data generated by the Qortex DTC engine is broadcast via TCP/IP. To capture this stream, a dedicated Python script (*trajectory_data.py*) was developed and executed within an Anaconda environment. The acquisition process performs three critical functions:

1. **JSON Streaming & Parsing:** The script ingests newline-delimited JSON packets containing the core kinematic parameters of detected objects, including unique Object IDs, timestamps, 3D coordinates (x, y, z), and velocity/acceleration vectors.
2. **Automated Archiving:** Raw tracking data is automatically serialized and stored. This decouples the data collection phase from the analysis, ensuring no data loss occurs during high-traffic periods.
3. **Visual Validation (Ground Truth):** Parallel to the LiDAR data stream, **OBS Studio** is employed to screen-capture the visual output of the Qortex interface. This serves as a secondary validation layer, allowing researchers to visually correlate the numerical trajectory data with observed real-world dynamics during the post-processing phase.

Due to the high frequency of acquisition, the resulting JSON datasets are voluminous and require optimization before analysis. A secondary Python processing pipeline was implemented to execute the following operations:

- **Data Segmentation:** Large datasets are fragmented into manageable time windows while strictly maintaining trajectory continuity for unique Tracking IDs.
- **Kinematic Extraction:** The script filters the dataset to isolate relevant road users, extracting essential kinematic information while discarding noise or static artifacts.
- **Format Transformation:** The filtered data is converted from hierarchical JSON structures into tabular formats (CSV/Excel). This transformation facilitates manual temporal synchronization and enables direct inspection of trajectory consistency.

This fully automated approach represents a significant advancement over traditional manual video analysis. By programmatically extracting timestamped coordinates, velocities (v_x, v_y), and accelerations, the workflow eliminates human error and provides the high-precision numerical baseline required for the subsequent computation of **Surrogate Safety Measures (SSMs)**.

The raw trajectory data acquired via the LiDAR sensor requires a structured post-processing phase to transition from discrete coordinate points to continuous kinematic profiles. The analysis specifically targets vehicle-pedestrian/cyclist interactions and is grounded in a relative reference system.

As illustrated in the conceptual diagram of a vehicle-pedestrian interaction below (fig. 3), the **Conflict Point (CP)**, defined as the exact geometric intersection between the vehicle and pedestrian trajectories, serves as the spatial origin ($x = 0$). Consequently, vehicle distances upstream of the CP are recorded as negative values.

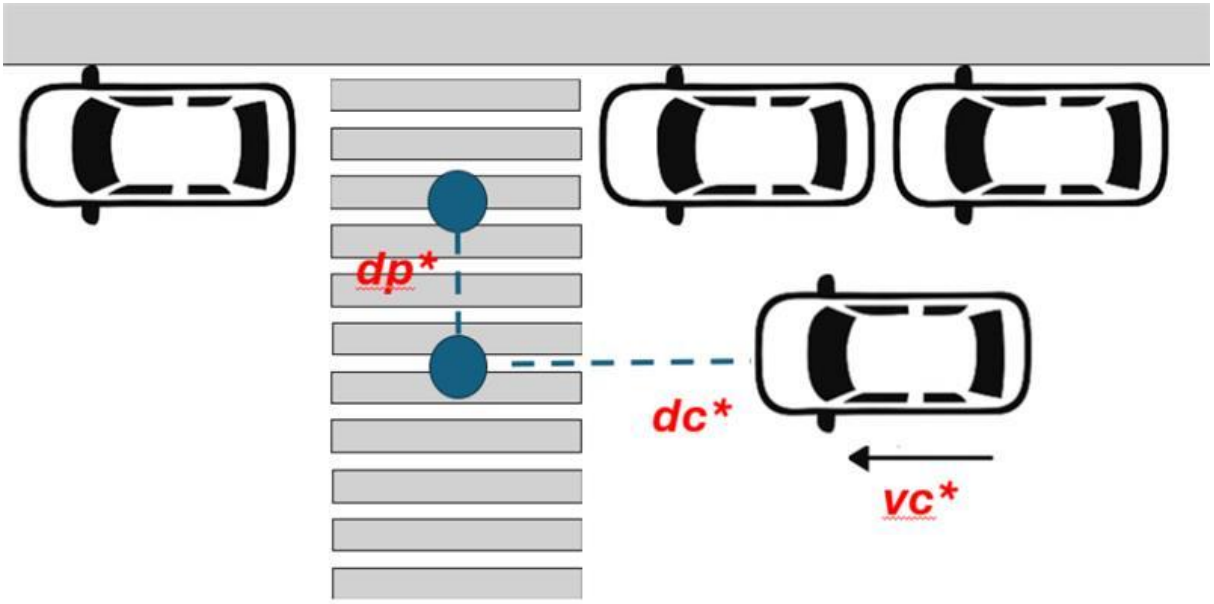

Fig. 3 — Example of parameters implemented for the calculation of the Surrogate Safety Measures (SSMs)

The geometric and kinematic reconstruction of the interaction is triggered by the identification of the **Pedestrian Gap Acceptance** instant (Miller, 1971; Troutbeck, 1992). This critical timestamp is defined as the moment when the pedestrian's distance from the conflict point becomes monotonically decreasing within a specific proximity threshold, denoted as dp^* (e.g., $2.5m - 3.0m$), signaling an unequivocal decision to initiate the crossing maneuver.

At this precise instant ($t = dp^*$), the system extracts the initial kinematic conditions of the approaching vehicle:

- $\boldsymbol{Vi}$ **(Initial Velocity):** The instantaneous speed of the vehicle at the moment of gap acceptance.
- $\boldsymbol{LVi}$ **(Initial Distance):** The longitudinal distance of the vehicle from the conflict point (typically a negative value indicating the approach phase).

These parameters define the vehicle configuration at the onset of the interaction and are explicitly represented in the speed–space profile (see figure below, fig. 4), where the vertical reference line associated with dp^* identifies the corresponding LVi and Vi.

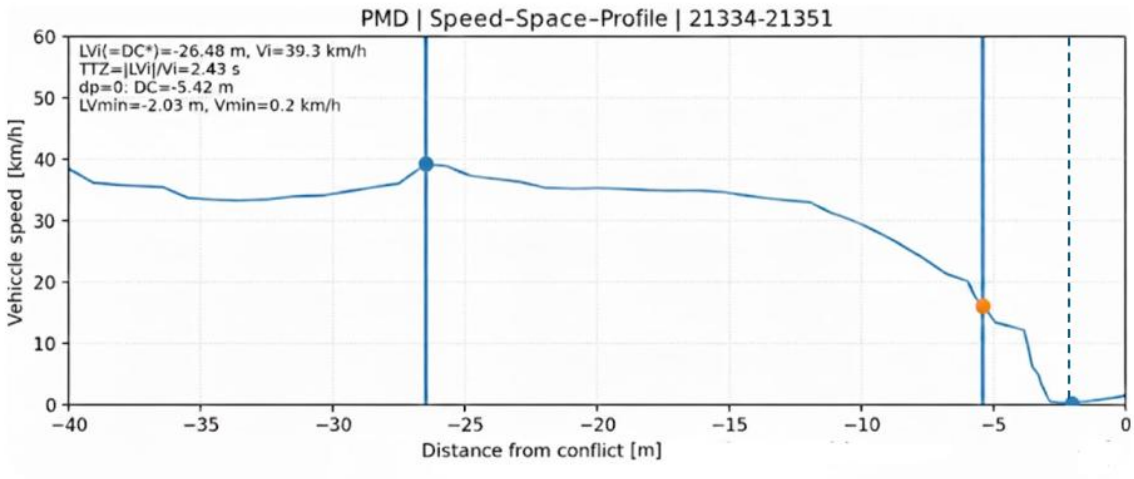

Fig. 4 — Example of a speed–space profile in relation to the distance from conflicts

Furthermore, continuous Speed–Space Profiles are generated for the spatial window extending from approximately $40m$ upstream to the conflict point. This representation allows for a direct visualization of the deceleration pattern as the vehicle approaches the crosswalk.

From these profiles, behavioral descriptors are derived, including:

- V_{min}: the minimum vehicle speed observed within the critical approach window (typically −20 m to 0 m);
- LV_{min}: the longitudinal position at which V_{min}occurs.

In addition, the vehicle configuration is explicitly evaluated at the instant when the pedestrian reaches the conflict point ($dp = 0$). At this timestamp:

- $L(dp = 0)$represents the longitudinal distance of the vehicle from the conflict point;
- $V(dp = 0)$represents the vehicle speed at the same instant.

Graphically, this condition corresponds to the vertical reference line marking the pedestrian arrival at the CP (visible in the figure 4), where the associated vehicle distance (DC at $dp = 0$) and the corresponding speed can be directly read from the speed–space profile.

Together, V_{min}, LV_{min}, $L(dp = 0)$, and $V(dp = 0)$distinguish between complete stops, pronounced yielding decelerations, and non-yielding maneuvers. Their graphical representation in the speed–space domain clarifies the geometric and physical meaning of the quantities dp^*, dc^*, Vi, and LVi, strengthening the interpretability of the subsequent surrogate safety analysis.

2.2.2 PoliTO and UniPD approach

The same hardware and software package described in Chapter 2.1, consisting of the M8-Prime Ultra LiDAR sensor as the primary data acquisition hardware and QORTEX DTC™ as the main raw point cloud data processing software (object detection, classification, and tracking), both provided by Quanergy Solutions, Inc., along with all required connection, power supply, and auxiliary components, was used in the Torino and Padova case studies.

A python script, in Jupyter Notebooks environment, were developed to:

1. Reorganize the timestamp-wise hierarchical JSON structures into tabular trajectory data (e.g., position, size, velocity, acceleration, and heading) stored in Pandas DataFrames for each detected road user.
2. Calculate the Instantaneous Time to Collision (ITTC) and its minimum value over the entire data collection period for each pair of detected road users.
3. Generate datasets describing interactions between different road user types, including vehicle–vulnerable road user (VRU) interactions (all VRU categories), vehicle–pedestrian, vehicle–cyclist, and cyclist–pedestrian.
4. Visualize road user interaction data, including conflict points and the corresponding trajectories, to identify hazardous locations within the investigated intersection

2.3 Surrogate Safety Measures

2.3.1 UniRomaTre approach

To quantify the risk level of each interaction, the methodology integrates a set of Surrogate Safety Measures (SSMs). These indicators are computed to assess both the temporal proximity of a potential collision and the intensity of the evasive action taken by the driver.

Starting from the filtered and temporally aligned trajectories, all SSMs were evaluated frame-by-frame (10 Hz) and subsequently synthesised at the interaction level using representative values (minimum or maximum). A unique conflict point was defined as the geometric intersection of the two trajectories. For each frame i, pedestrian and vehicle distances from the conflict point $d_p(i)$, $d_c(i)$, and instantaneous speeds $v_p(i)$, $v_c(i)$, were computed. The analysis was restricted to the pre-encroachment phase, up to the interaction time t_{int}.

The adopted SSMs are listed below.

- **Time to Collision (TTC_{min}) — Ni et al., pedestrian crossing first** $\left(t_p < t_c \right)$

  Nominal arrival times are defined as $t_p(i) = d_p(i)/v_p(i)$and $t_c(i) = d_c(i)/v_c(i)$. Following Ni et al. (Ni et al., 2016), user dimensions are introduced via pedestrian width $w_p$and vehicle length w_c. In the case where the pedestrian crosses first $\left(t_p < t_c \right)$, the frame-based TTC is computed as:

$$TTC_i = \max \left(\frac{d_p(i) + w_p}{v_p(i)}, \frac{d_c(i)}{v_c(i)} \right)$$

The representative interaction-level value is:

$$TTC_{min} = \min_i (TTC_i)$$

- **Gap Time (GT_{min}) — Ni et al., pedestrian crossing first** $\left(t_p < t_c \right)$

  For the same crossing order $\left(t_p < t_c \right)$, the frame-based Gap Time is computed as (Ni et al., 2016; Gagliardi et al., 2024):

$$GT_i = \left| \frac{d_p(i) + w_p}{v_p(i)} - \frac{d_c(i)}{v_c(i)} \right|$$

The interaction-level indicator is:

$$GT_{min} = \min_i (GT_i)$$

- **Post-Encroachment Time (PET)**

  PET is defined as the temporal separation between the instant when the first user clears the conflict point and the instant when the second user reaches it (Ni et al., 2016; Gagliardi et al., 2024):

$$PET = t_{in,2} - t_{out,1}$$

It is computed once per interaction and interpreted together with the crossing order.

- **Maximum Required Deceleration MAxD**

  The severity of the potential evasive manoeuvre is quantified by the maximum theoretical deceleration required for the vehicle to stop before the conflict point, assuming uniform braking (FHWA, 2009):

$$MaxD_i = \frac{v_c(i)^2}{2\, d_c(i)}, MaxD = \max_i (MaxD_i)$$

- **Proportion of Stopping Distance (PSD_{min})**

  PSD quantifies the stopping margin (Allen, 1978) assuming a reference deceleration a, adopted according to AASHTO guidelines and set equal to $a = 3.4$ m/s^2:

$$PSD_i = \frac{2\, a\, d_c(i)}{v_c(i)^2}, PSD_{min} = \min_i (PSD_i)$$

- **Time To Zebra (TTZ)**

  TTZ is an event-based indicator computed at the frame in which $d_p(t)$begins to decrease monotonically, interpreted as the onset of the pedestrian's crossing decision (Bella et al. 2021). Denoting by $d_c^*$and $v_c^*$the vehicle distance and speed at that instant:

$$TTZ = \frac{d_c^*}{v_c^*}$$

TTZ captures the temporal window available to the pedestrian at the decision moment, separating the decision phase from the subsequent vehicle response.

2.3.2 PoliTO and UniPD approach

Time to collision (TTC), was selected as the primary conflict metric. Figure , adopted from (Tarko, 2019), demonstrates the calculation of the TTC and the potential crash point. Two vehicles move along straight paths with velocities V_1 and V_2. The vehicles are on a collision course if there is a line parallel to the relative velocity $\Delta V = V_2 - V_1$ that intersects both vehicle bodies. The shortest segment P_1P_2, parallel to ΔV , connects potential collision points $P_1$and P_2. The intersection of the lines drawn parallel to the V_1 and V_2 from P_1 and P_2, respectively, defines the potential crash point, or conflict point (CP) within the area. The length of the line segment P_1P_2 is the current distance to collision D, and the current time to collision is:

$$TTC = \frac{D}{||\Delta V||}$$

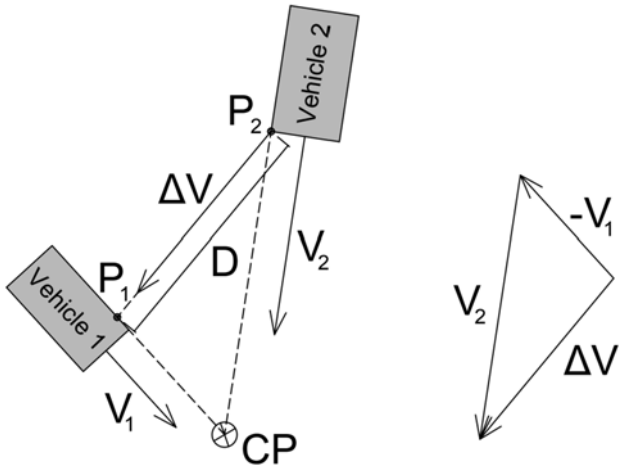

Figure 5 - Time to collision with consideration of the points of physical contact at collision of vehicles

At each timestamp, the current speed vector of each detected road user, defined by both magnitude and direction, is assumed to represent their future motion. Under this assumption and given the current positions and headings and taking into account the dimensions of the boxes representing the vehicles, potential collision courses are projected. When a collision course is identified, the instantaneous time to collision (ITTC) is calculated for all pairs of road users present at that timestamp using the equation and logic described above. The minimum ITTC value between two road users is used as a severity indicator of their interaction. Severity is quantified using an exceedance metric defined as $t_c - \min ITTC$, where t_c is a critical TTC threshold. The t_c is set to 3 seconds for this study, and interactions with a $\min ITTC$ below this threshold are classified as conflicts for analysis.

3 Case Study 1: Rome

The case study selected examines a complex urban intersection in Rome, Italy. This location represents a critical node within the municipal road network, characterized by significant challenges regarding safety performance, operational efficiency, and the intrinsic complexity of the surrounding urban environment. The selection of this site was driven by a preliminary consultation phase with the Mobility Department of the Municipality of Rome and *Roma Servizi per la Mobilità* (RSM), alongside the accident data analysis detailed in Deliverable 1. Furthermore, the identification of specific monitoring segments resulted from a comprehensive methodological approach that integrated preliminary site inspections, traffic flow assessments, and structured stakeholder consultations. The direct engagement of municipal representatives and RSM, the agency overseeing traffic safety and mobility planning, was instrumental not only in validating the technical relevance of the chosen segments but also in ensuring that the monitoring activities align with both ongoing and prospective municipal safety planning initiatives.

The area is characterized by highly mixed land use, including residential buildings, commercial activities, educational facilities, and several public transport stops. As a result, the intersection functions as a strategic mobility hub, connecting multiple radial and tangential routes within the north-western quadrant of Rome.

The intersection accommodates a heterogeneous and continuous flow of road users: private motor vehicles, public buses, motorcycles, bicycles, and a substantial number of pedestrians. The study area is an unsignalized intersection regulated exclusively through vertical and horizontal signage, including a stop sign on the minor road relative to the main traffic stream. Despite the absence of traffic lights, the site includes marked pedestrian crossings. Nevertheless, it has been repeatedly reported as a hotspot for unsafe behaviors, including illegal pedestrian crossings, non-compliance with right-of-way rules, and critical interactions among different categories of road users (Bella; Nobili, 2020).

The selection of this location as a pilot site for LiDAR-based monitoring is motivated by several factors:

- the high potential for multi-user conflicts;
- the pronounced heterogeneity of traffic flows;
- the recurrent safety concerns highlighted in municipal road safety assessments;

- the presence of visual obstructions caused by parked vehicles, vegetation, and urban furniture, which complicate both user behavior and traditional observation methods.

In addition to the intrinsic complexity of the selected site, the case study was supported by a comprehensive LiDAR-based field data collection campaign, meticulously planned to acquire a statistically robust sample of road user interactions. The overarching objective was to enable a detailed safety analysis grounded in surrogate safety measures (SSMs), which require a sufficiently large and diverse dataset to capture the full spectrum of potential conflict scenarios.

To this end, multiple acquisition sessions were conducted over several days and time windows, encompassing both peak and off-peak periods. This temporal stratification was essential to ensure the inclusion of a wide range of traffic conditions, behavioral dynamics, and environmental contexts. The campaign was designed not only to maximize the representativeness of the observed interactions but also to capture the variability in user behavior that typically emerges under different levels of traffic demand and exposure.

Field data collection was carried out across three strategically selected segments within the broader study area, as illustrated in Figure 6. Each corresponding to a critical component of the intersection's functional layout:

- **Via Prisciano**, (indicated by the cyan marker): a feeder road with significant vehicular inflow and frequent pedestrian crossings;
- **Piazza delle Medaglie d'Oro** (indicated by the red marker): the central node of the intersection, characterized by high multimodal density and complex maneuvers;
- **Via delle Medaglie d'Oro** (indicated by the green marker): a major arterial corridor with sustained traffic volumes and recurrent interactions between motorized and vulnerable road users.

Figure 6 - LiDAR positions at the Case Study intersection

Detailed mappings of the relevant maneuvers, expressed as kinematic trajectories, are presented in Figure 7.

Figure 7 - Maneuvers investigated within the intersection framework

To ensure a robust analysis of surrogate safety measures, such as Time to Collision (TTC), Post-Encroachment Time (PET), and speed-based conflict indicators, a targeted data acquisition campaign was conducted across the three identified segments. Each campaign employed fixed-position LiDAR sensors to capture high-resolution, real-time spatiotemporal data on the interactions between vehicles and Vulnerable Road Users (VRUs). The resulting dataset provides a comprehensive empirical foundation for assessing conflict typologies and developing context-sensitive safety interventions.

Figure 8 illustrates the deployment implemented during the first field campaign in Via Prisciano, detailing the positioning of the LiDAR sensor and the battery-powered acquisition station, which allowed for approximately four hours of continuous data acquisition.

Figure 8 - Field Campaign 1 (Via Prisciano): LiDAR deployment and mobile acquisition station with Prof. Bella (ARCADE PI).

Figure 9 presents the layout of the instrumentation and sensor placement for the second field campaign, conducted at the central node of Piazza delle Medaglie d'Oro.

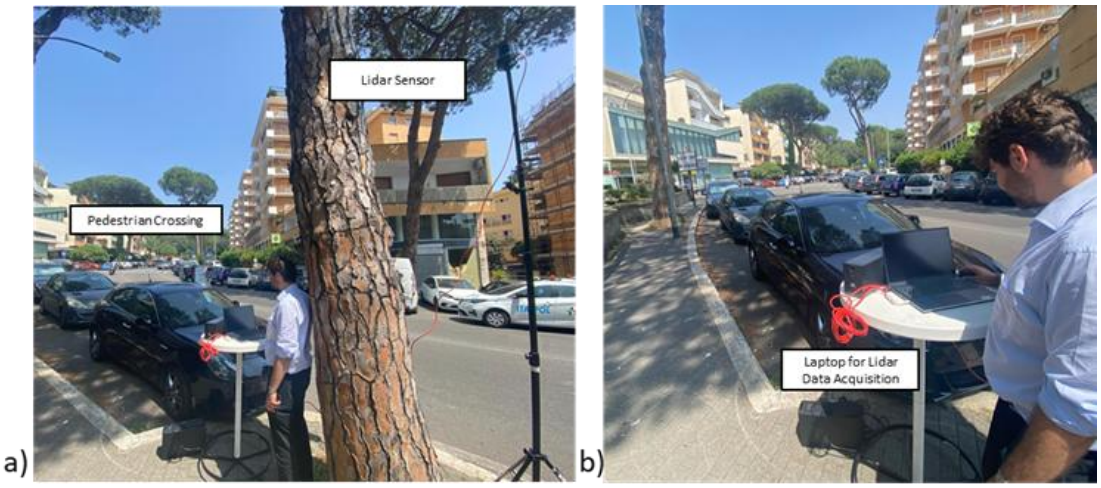

Figure 9 - Field Campaign 2 (Piazza delle Medaglie d'Oro): (a) experimental setup and sensor positioning; (b) real-time trajectory acquisition of a motorcycle.

Finally, Figure 10 documents the sensor configuration and deployment strategy for the third field campaign, carried out along the Via delle Medaglie d'Oro arterial corridor. The trajectories extracted from these three datasets serve as the primary input for the maneuver analysis presented in the following sections.

Figure 10 - Field Campaign 3 (Via delle Medaglie d'Oro): (a) experimental setup and sensor positioning; (b) real-time detection of vehicle–pedestrian interactions.

Building on this foundation, the structured and multi-scalar design of the data collection campaign significantly enhances the analytical depth of the case study. It supports the identification of recurrent behavioural patterns, the quantification of exposure to risk maneuvers, and the assessment of safety performance under varying operational conditions.

Moreover, the methodological framework adopted for the field campaign was conceived to be both replicable and scalable, offering a transferable reference methodology for the deployment of LiDAR-based monitoring systems in similarly complex urban environments. This approach contributes to the advancement of proactive, data-driven safety diagnostics and underpins the integration of innovative sensing technologies into broader strategies for sustainable, inclusive, and resilient urban mobility planning.

3.1 Empirical Reconstruction of Interaction Dynamics

The analysis of vehicle–pedestrian interactions at sites AP1 (Via Prisciano) and AP2 (Piazzale delle Medaglie d'Oro) was conducted through high-resolution LiDAR trajectory tracking, facilitating the reconstruction of longitudinal velocity–distance profiles (v_x). Figure 11 illustrates the resulting velocity–distance profiles for Via Prisciano and Piazzale delle Medaglie d'Oro (AP1 and AP2) site, highlighting the high variability in speed modulation across different interaction events.

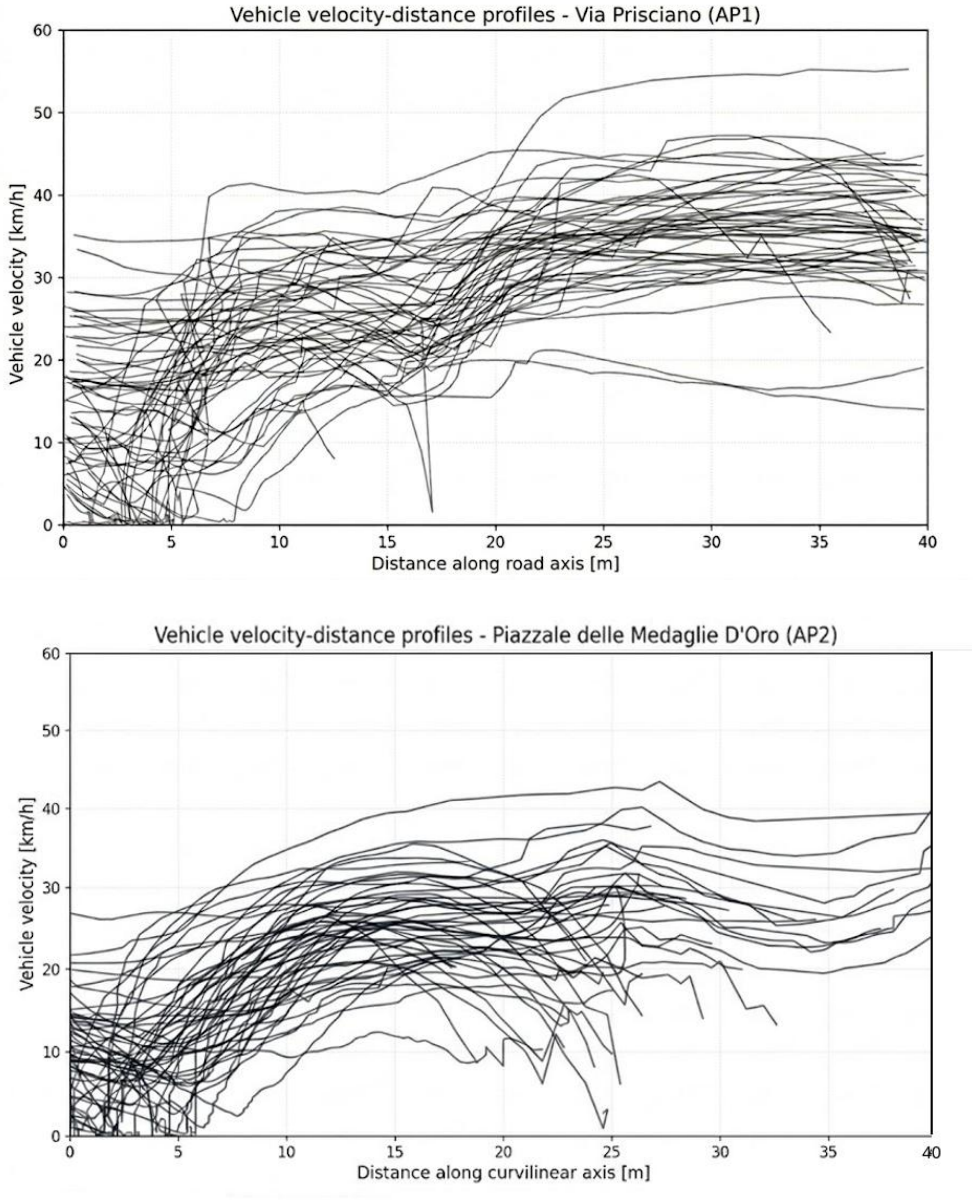

Figure 11 – Vehicle velocity-distance profiles (AP1 and AP2)

This approach enables a process-based interpretation of traffic safety. Rather than characterizing interactions through isolated point-based indicators, each event is interpreted as a dynamic process, progressively unfolding along the vehicle's approach trajectory toward the crosswalk. The integrated computation of

kinematic ($\Delta V, MaxD$), spatial (PSD), and temporal indicators (TTC, PET, TTZ), combined with an analysis of the residual speed at the conflict point $V\ (dp = 0)$, reveals that potential severity cannot be attributed to a single parameter. Instead, it emerges from the interplay between:

- The initial spatiotemporal configuration (LV_i, V_i, TTZ);
- The structure of longitudinal modulation ($\Delta V, slope\ of\ v(x), PSD, MaxD$);
- The residual outcome at the point of conflict ($V(dp = 0), TTC\_min, PET$).

The initial speed (V_i) alone demonstrated limited discriminative power across varying behavioral configurations. Conversely, the initial longitudinal distance (LV_i), and, by extension, the Time to Zebra ($TTZ = LV_i/V_i$), plays a structural role in shaping the interaction. Under reduced TTZ conditions (representing a compressed spatiotemporal margin), several phenomena were observed:

- Deceleration becomes spatially concentrated near the crosswalk;
- Peak deceleration ($MaxD$) increases;
- PSD decreases, reflecting a compressed utilization of the available stopping space;
- Greater dispersion in the slopes of speed profiles becomes evident.

These findings confirm that TTZ is not merely a temporal metric, but a structural determinant governing the dynamic organization of speed adaptation. Consequently, safety must be interpreted as an emergent property of the entire approach trajectory, rather than as a discrete event defined by the exceedance of a single threshold indicator.

3.2 Behavioural Clustering: Emerging Response Strategies

The clustering analysis of the reconstructed velocity–distance profiles identified three recurrent and physically interpretable response strategies, which reflect distinct behavioral patterns in vehicle-pedestrian interactions.

Cluster 1 – Full or Near-Stop Maneuvers

This cluster is characterized by the following dynamics (Figure 12):

- **Residual Velocity:** $V(dp = 0)$ approaching zero, indicating a complete or near-complete cessation of movement at the conflict point.
- **Deceleration Intensity:** High MaxD values, reflecting a marked reduction in kinetic energy as the vehicle approaches the pedestrian crossing.
- **Deceleration Structure:** A consistent and anticipatory deceleration profile, suggesting a proactive yielding strategy.

This behavioral configuration is associated with a reduced residual conflict severity, as the vehicle-pedestrian interaction is managed through early and controlled speed modulation.

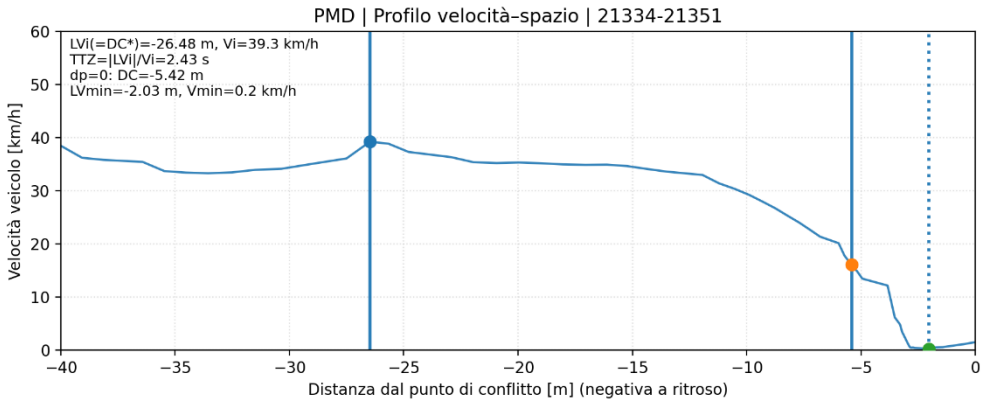

Figure 12 – speed-space profile Cluster 1

Cluster 2 – Marked Deceleration without Full Stop

This cluster represents a transitional behavioral configuration, situated between active yielding and minimal speed modulation. It is characterized by the following dynamics (Figure 13):

- **Speed Reduction:** A significant yet spatially distributed reduction in velocity, resulting in high ΔV values across the approach trajectory.
- **Deceleration Intensity:** Intermediate $MaxD$ values, indicating a controlled reduction in speed that lacks the abruptness observed in Cluster 1.
- **Residual Outcome:** A moderate residual speed at the conflict point, suggesting that the driver maintains sufficient momentum to proceed without coming to a complete or near-complete stop.

This configuration reflects a cautious, yet non-evasive, approach, where the driver adjusts their speed in response to the pedestrian presence without fully relinquishing the right-of-way.

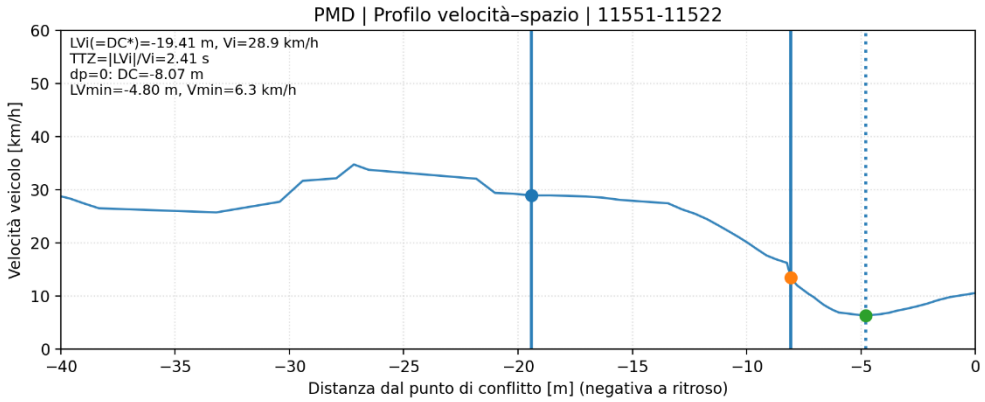

Figure 13 - speed-space profile Cluster 2

Cluster 3 – Weak Modulation

This behavioral configuration is characterized by a "low-effort" approach to interaction, where the driver implements minimal modifications to their kinematic state. It is defined by the following dynamics (Figure 14):

- **Speed Variation:** Limited velocity reduction throughout the approach, resulting in low ΔV values.
- **Deceleration Intensity:** Significantly lower $MaxD$ values compared to the other clusters, indicating a lack of proactive speed adaptation.
- **Residual Outcome:** Higher residual speed at the conflict point, reflecting the driver's tendency to maintain momentum despite the presence of pedestrians.

Although the peak deceleration values in this cluster are the lowest among the three groups, the combination of non-negligible residual speed and a reduced spatial margin for maneuvering increases exposure to potentially critical safety configurations. This finding demonstrates that the severity of an interaction is primarily dictated by the structure and timing of deceleration, rather than by absolute speed levels alone, thereby reinforcing the importance of analyzing the entire approach trajectory.

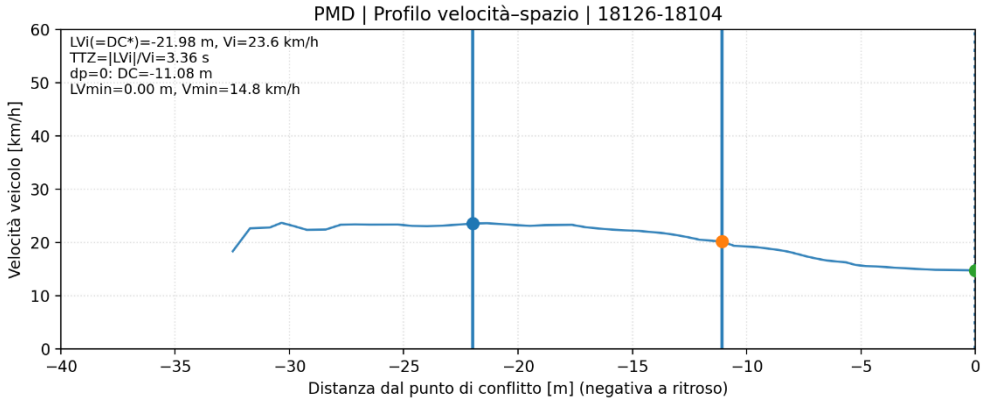

Figure 14 - Speed-space profile Cluster 3

3.3 Comparison of Behavioral Clusters between the Two Crosswalks

The comparison of the behavioral clustering results obtained at the two analyzed crosswalks highlights that the response strategies identified through the classification of velocity–distance profiles exhibit a consistent structural pattern across both sites, while showing systematic differences in the values and distributions of the analyzed indicators. These variations appear closely related to the geometric and perceptual characteristics of the two infrastructural contexts.

Comparison of Deceleration Intensity (MaxD)

The boxplots of the maximum deceleration (MaxD) variable, presented in Figure 15, display a clear and consistent progression across the three behavioral clusters in both sites, confirming the coherence of the velocity–distance profile classification.

In Cluster 1 (full or near-stop maneuvers), the highest MaxD values are observed, indicating a strong and concentrated deceleration response occurring during the final phase of the vehicle approach to the crosswalk. In Cluster 2, the values are generally lower and more dispersed, reflecting a substantial but more spatially distributed reduction in speed. In Cluster 3, deceleration levels are noticeably lower, consistent with a weak modulation of speed.

A systematic difference emerges when comparing the two sites: MaxD values are generally higher in AP1 (Via Prisciano) than in AP2 (Piazzale delle Medaglie d'Oro). This pattern is consistent with the geometric characteristics of the two contexts. In Via Prisciano, the straight alignment and wider carriageway facilitate higher approach speeds, which consequently lead to stronger deceleration once the driver initiates a yielding maneuver. In contrast, the right-hand curved approach in Piazzale delle Medaglie d'Oro results in generally lower approach speeds and a more gradual vehicle response, producing lower peak deceleration values.

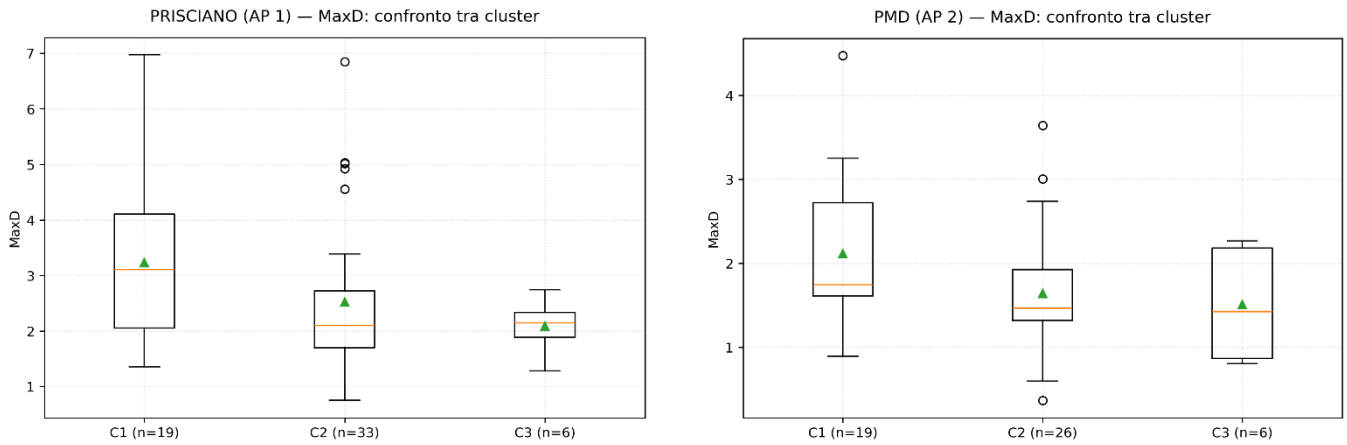

Figure 15 - Comparison of Maximum Deceleration (MaxD) distributions across identified behavioral clusters at AP1 and AP2

Spatial Distribution of Deceleration (PSD)

A consistent behavioral pattern is also evidenced by the analysis of the Proportion of Stopping Distance (PSD) boxplots, presented in Figure 16.

Across both sites, a structured progression is observed across the behavioral clusters. Cluster 1 exhibits the lowest PSD values, indicating that deceleration is spatially concentrated within a compressed segment of the available approach distance, typically in the immediate vicinity of the crosswalk. In contrast, Cluster 3 presents higher PSD values, reflecting a more gradual and distributed modulation of speed throughout the entire approach. Cluster 2 occupies an intermediate position, demonstrating a balanced spatial distribution of deceleration.

A comparative analysis between the two crosswalks reveals that AP1 (Via Prisciano) consistently displays lower PSD values than AP2 (Piazzale delle Medaglie d'Oro). This suggests that, at Via Prisciano site, speed reduction tends to be highly localized and intensified as the vehicle approaches the crossing. Conversely, at Piazzale delle Medaglie d'Oro, velocity modulation appears more progressively distributed along the approach trajectory. This discrepancy aligns with the distinct geometric configurations of the two sites: the curved alignment at AP2 naturally encourages earlier and more gradual speed adjustments compared to the straight, high-visibility approach characteristic of AP1.

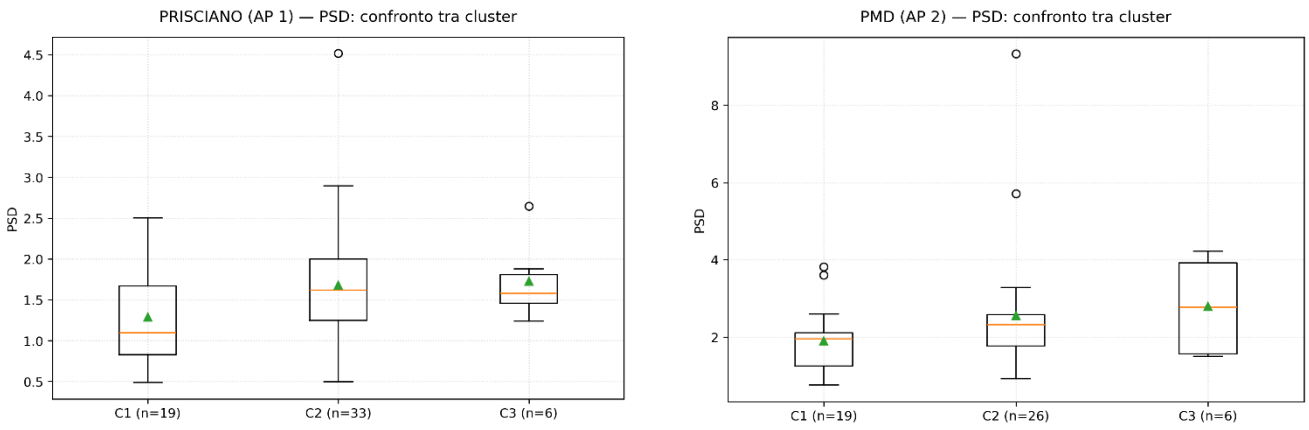

Figure 16 - Comparison of Proportion of Stopping Distance (PSD) distributions across identified behavioral clusters at AP1 and AP2

Residual Speed at the Conflict Point (V(dp=0))

The comparative analysis of the residual speed at the conflict point, V(dp=0), presented in Figure 17, further reinforces the clear differentiation between the three behavioral clusters.

Across both sites, the clusters exhibit distinct kinematic outcomes:

- **Cluster 1:** Residual speeds are consistently close to zero, reflecting a proactive, full-yielding behavior.
- **Cluster 2:** This configuration is characterized by moderate residual speeds, indicating a controlled approach that retains some kinetic energy.
- **Cluster 3:** This group displays the highest V(dp=0) values, confirming limited speed modulation and a consequently higher exposure to potentially critical interaction configurations.

However, notable differences emerge regarding the spatial positioning of the speed reduction process. In AP2 (Piazzale delle Medaglie d'Oro), the residual speeds observed in Cluster 3 are generally associated with a delayed velocity reduction, often concentrated in the immediate vicinity of the crosswalk. In contrast, at AP1 (Via Prisciano), the enhanced visibility provided by the straight road alignment enables drivers to initiate speed modulation earlier. Nevertheless, this earlier initiation does not always ensure a substantial reduction in residual speed for the least reactive behavioral configurations, underscoring the complex relationship between infrastructure, driver perception, and kinematic response.

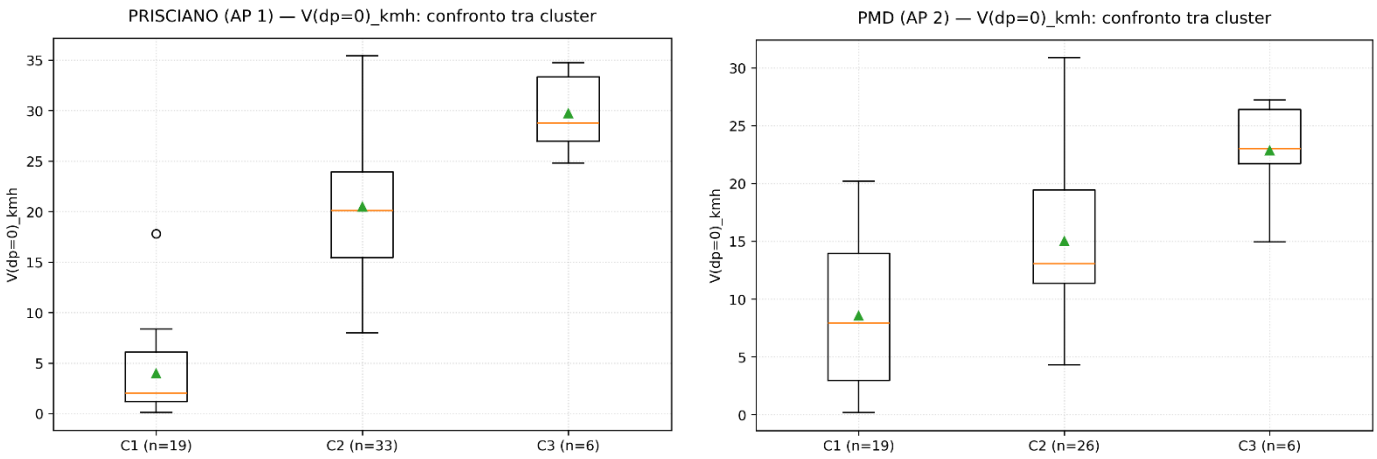

Figure 17 - Comparison of residual speed at the conflict point V(dp=0) across identified behavioral clusters at AP1 and AP2

In summary, the comparison between the two study sites confirms that the behavioral clustering structure remains consistent across different urban contexts, thereby supporting the robustness of the classification methodology based on velocity–distance profiles. While the identified response strategies are structurally stable, the observed differences primarily concern the intensity and spatial distribution of the dynamic responses.

At Via Prisciano (AP1), the straight road alignment and wider carriageway facilitate higher approach speeds. This geometric configuration leads to more intense deceleration, which is typically concentrated within a compressed spatial segment as the vehicle nears the crosswalk, as evidenced by higher MaxD values and lower PSD metrics.

Conversely, at Piazzale delle Medaglie d'Oro (AP2), the curved approach and restricted visibility induce lower average speeds but encourage a more progressive velocity modulation. This results in higher PSD values and lower peak deceleration, reflecting a more distributed speed adaptation process.

These findings confirm that the potential severity of vehicle–pedestrian interactions cannot be attributed solely to absolute speed levels. Instead, severity must be interpreted as the outcome of the overall dynamic configuration of the approach process, which is fundamentally influenced by the geometric and perceptual characteristics of the site. This holistic perspective underscores the necessity of moving beyond discrete indicators toward process-based safety diagnostics in urban mobility planning.

3.4 Stratification by TTZ Classes: Margin-Driven Criticality

Stratification based on Time to Zebra (TTZ) thresholds further clarifies how safety performance fluctuates when interactions are initiated under varying spatiotemporal margins. This analysis reveals a distinct dichotomy in driver behavior depending on the initial margin availability:

- **Low TTZ Conditions (Compressed Margin):** When TTZ is low, the available adaptation interval is severely constrained. Consequently, longitudinal modulation becomes spatially compressed, resulting in significantly higher MaxD values and lower PSD metrics (Figure 18). In these scenarios, deceleration is predominantly localized in the immediate proximity of the conflict area .
- **High TTZ Conditions (Extended Margin):** Conversely, when TTZ is high, deceleration is more progressive, allowing for speed adaptation to be distributed over a more extensive spatial segment, which leads to lower peak deceleration values.

This evidence supports a hierarchical interpretation of interaction severity, wherein the evolution of a potential conflict is defined by three sequential stages:

- **Initial Configuration (LV_i, V_i, TTZ):** This phase establishes the baseline spatiotemporal margin available for the driver to process the interaction.
- **Longitudinal Response Structure ΔV, slope of v(x), PSD, MaxD):** This stage describes the operational application of the margin, characterizing the driver's strategy in modulating speed.
- **Residual Outcome (V(dp=0), TTC, PET):** This represents the final kinematic state, manifesting as the culmination of the preceding behavioral choices.

Ultimately, potential severity arises from the co-occurrence of a reduced initial margin, a high spatial concentration of deceleration, and a non-negligible residual speed at the crosswalk. This framework confirms that safety is not an isolated state but an emergent property of the entire interaction process, highly sensitive to the initial margin of engagement.

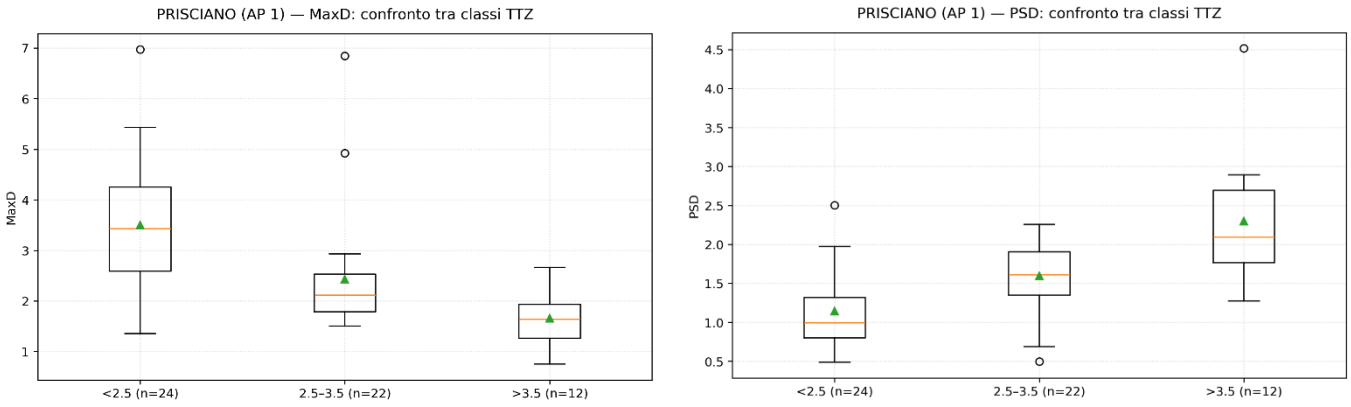

Figure 18 - Stratification of kinematic indicators by TTZ classes at Via Prisciano (AP1): Maximum Deceleration (MaxD) and Proportion of Stopping Distance (PSD)

3.5 Geometry-Driven Differences between AP1 and AP2

The comparative analysis reveals systematic behavioral differences between the two study sites, which are intrinsically linked to their respective geometric configurations. These findings demonstrate that roadway geometry influences not only absolute speed levels but, more critically, the structural organization of yielding behavior (Figure 19).

AP1 – Straight, Wide Carriageway

The configuration of Via Prisciano facilitates higher approach speeds and creates an environment where behavioral strategies are more sharply defined. Key kinematic characteristics include:

- **Deceleration Intensity:** Higher average MaxD values, indicating more forceful braking maneuvers.
- **Spatial Compression:** Lower PSD values, suggesting that deceleration is concentrated within a narrow spatial segment.
- **Cluster Separation:** A more pronounced distinction between behavioral clusters, reflecting a clear trade-off between yielding and non-yielding strategies.

In this context, potential safety criticality is primarily associated with the intensity and spatial compression of deceleration maneuvers.

AP2 – Curved Approach with Reduced Visibility

The right-hand curvature at Piazzale delle Medaglie d'Oro introduces greater perceptual complexity, leading to distinct kinematic patterns:

- **Velocity Modulation:** Lower mean approach speeds compared to AP1.
- **Deceleration Distribution:** Higher PSD values, reflecting a more progressive, albeit sometimes delayed, deceleration process.
- **Interaction Timing:** The spatial location of minimum velocity (LV_{min}) is typically closer to the crosswalk, influenced by the limited sight distance inherent in the curved geometry.

Here, interaction criticality is more strongly associated with delayed modulation and the spatial positioning of the vehicle's minimum speed, rather than with the peak magnitude of deceleration.

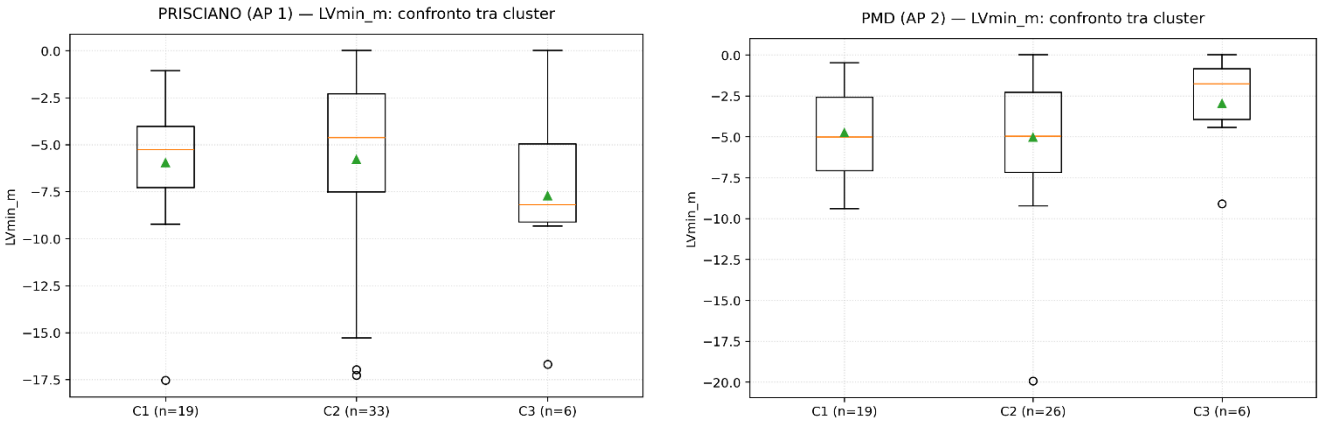

Figure 19 - Comparative analysis of kinematic indicators across behavioral clusters at AP1 and AP2

3.6 Evidence-Based Translation into Design Scenarios

The proposed design scenarios represent a direct operational translation of the empirical findings derived from the trajectory-based analysis. By adopting the hierarchical framework illustrated in Figure 20, which links initial configurations to residual conflict outcomes, the design interventions target specific phases of the vehicle-pedestrian interaction process.

The primary evidence-to-design correspondences are structured as follows:

- **Reduction of Effective Lane Width (4.9 m → 3.5 m):** This intervention structurally modifies approach speed regimes, effectively enlarging the available adaptation margins for drivers.
- **Installation of Pedestrian Refuge Islands:** This strategy facilitates a more progressive spatial distribution of deceleration, effectively reducing the behavioral compression observed near the conflict point.
- **Raised Crosswalk Implementation:** By introducing a vertical geometric constraint, this measure directly addresses the residual speed at the conflict area (V(dp=0)).
- **Comprehensive Carriageway Reconfiguration:** This approach induces perceptual and behavioral adaptation by imposing consistent geometric constraints throughout the approach trajectory.

Crucially, the proposed scenarios are not solely derived from traditional safety inspections or historical crash data. Instead, they are quantitatively grounded in observed dynamic interaction patterns and surrogate safety measures extracted from high-resolution LiDAR-based trajectory monitoring. This integration demonstrates the methodological added value of proactive, trajectory-based safety analysis in supporting evidence-based urban design interventions, moving towards a more resilient and inclusive mobility environment.

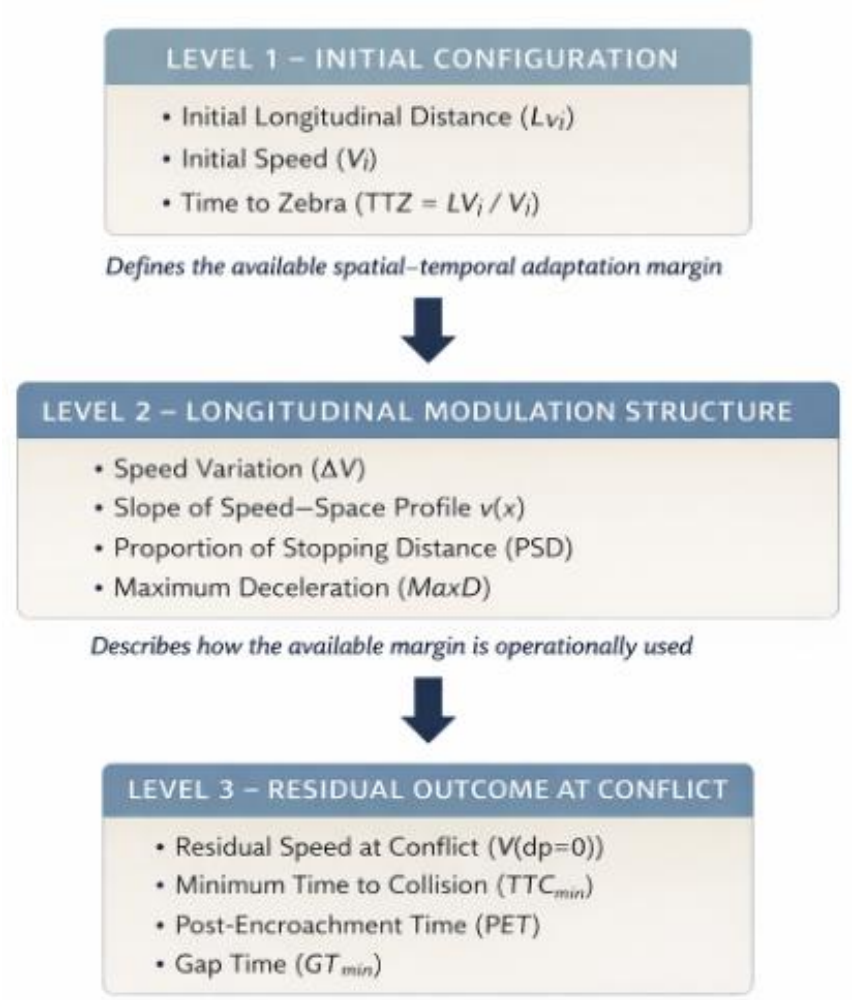

Figure 20 - Comparative Hierarchical framework for pedestrian-vehicle interaction analysis

4 Case Study 2: Turin

Case Study 2 was conducted at the intersection of Corso Castelfidardo and Corso Vittorio Emanuele II in Turin. Data collection was carried out in multiple sessions across different days of the week to capture potential temporal patterns. Due to the large size of the intersection, each data collection session focused on one of the two previously identified hazardous locations based on historical crash data. A separate sensor was deployed at each location to enable parallel data collection and reduce the overall survey time. Figure illustrates the investigated intersection and the spatial distribution of VRU-involved crash locations, highlighting the two focus areas identified through crash clustering analysis. In total, about 11 hours of data were collected for this case study (5 hours at Location 1 and 6 hours at Location 2). Table 1 summarizes the timing and duration of the data collection sessions, and the observation results are presented in the figures that follow.

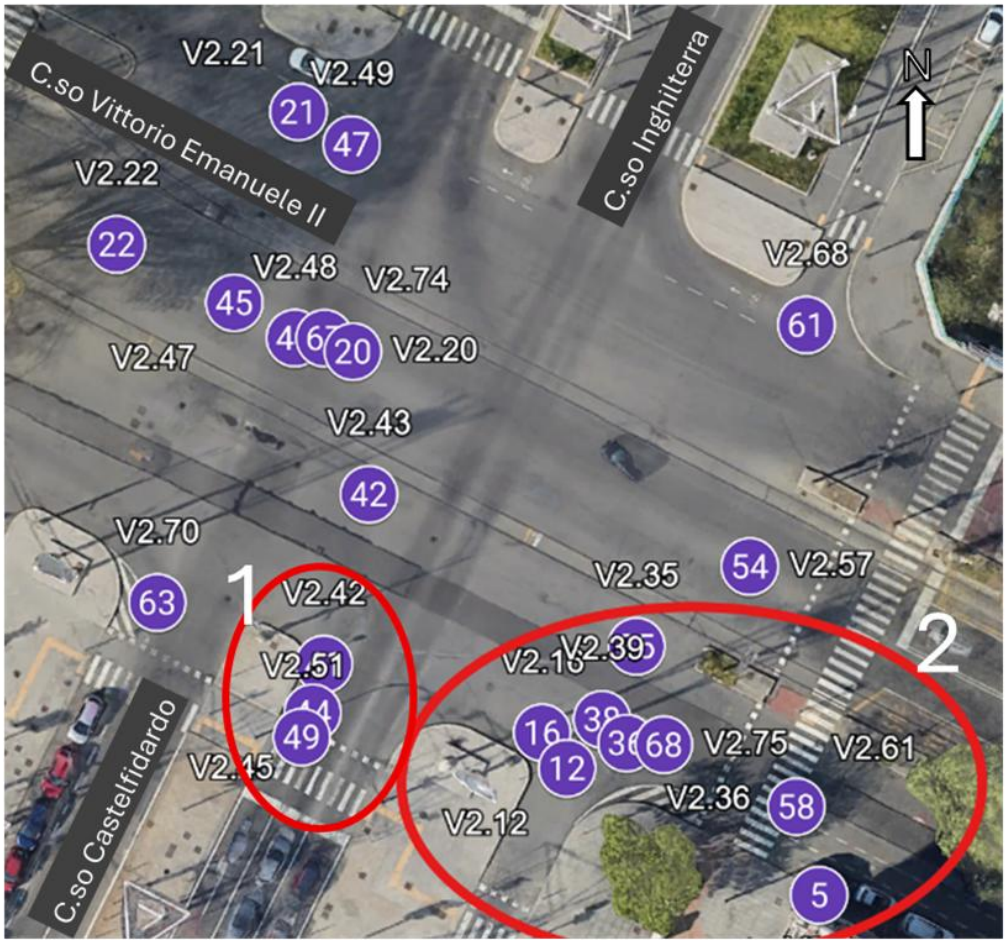

Figure 21 - Corso Castelfidardo - Corso Vittorio Emanuele II Intersection, Turin

Table 1 - Time and duration of the data collection sessions (Turin)

Location	Record	Day	Starting Time	Duration (mm:ss)
Location 1	Rec 1	1	11:56	15:04
	Rec 2		12:25	15:08
	Rec 3		12:42	19:20
	Rec 4		13:03	15:24
	Rec 5		13:40	15:13
	Rec 6		13:55	18:00
	Rec 7		14:15	18:13
	Rec 8		14:37	14:57
	Rec 9		14:52	15:20
Location 2	Rec 10	2	12:53	15:09
	Rec 11		13:08	16:05
	Rec 12		13:24	15:28
	Rec 13		13:41	15:02

	Rec 14		13:56	15:08
	Rec 15		14:20	16:46
	Rec 16		14:37	15:28
	Rec 17		14:52	15:22
	Rec 18		15:08	15:47
	Rec 19		15:23	15:53
	Rec 20		15:39	15:02
Location 1	Rec 21	3	12:09	20:25
	Rec 22		12:30	16:01
	Rec 23		12:46	15:11
	Rec 24		13:01	15:11
	Rec 25		13:28	15:11
	Rec 26		13:43	17:23
	Rec 27		14:00	15:03
	Rec 28		14:16	15:07
	Rec 29		14:31	15:28
	Rec 30		14:47	15:16
Location 2	Rec 31	3	12:26	15:29
	Rec 32		12:41	14:41
	Rec 33		12:56	15:55
	Rec 34		13:12	15:30
	Rec 35		13:28	14:55
	Rec 36		13:42	17:15
	Rec 37		13:59	14:50
	Rec 38		14:14	22:24
	Rec 39		14:36	15:32
	Rec 40		14:52	13:53
	Rec 41		15:06	15:14

Figure and Figure display all recorded trajectories and the calculated conflict points for Locations 1 and 2, respectively.

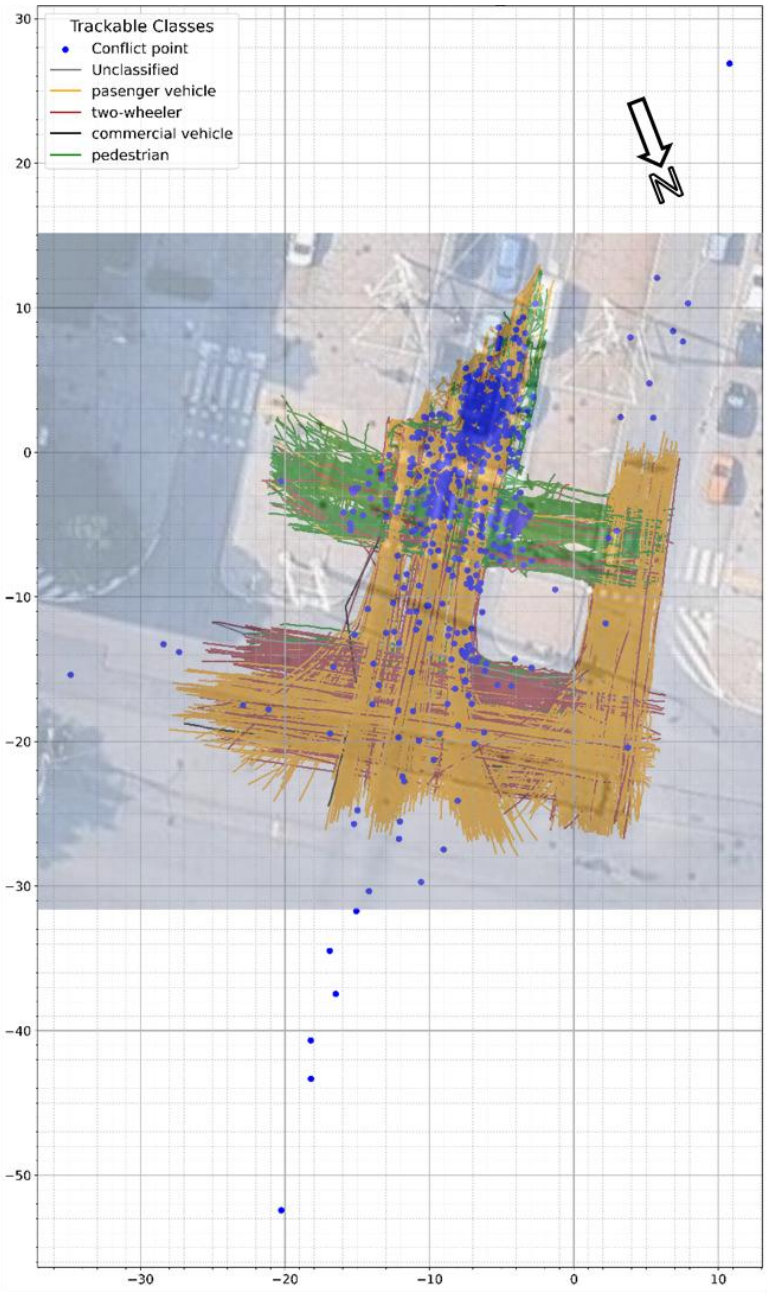

Figure 22 - All trajectory and conflict points, Location 1, Turin

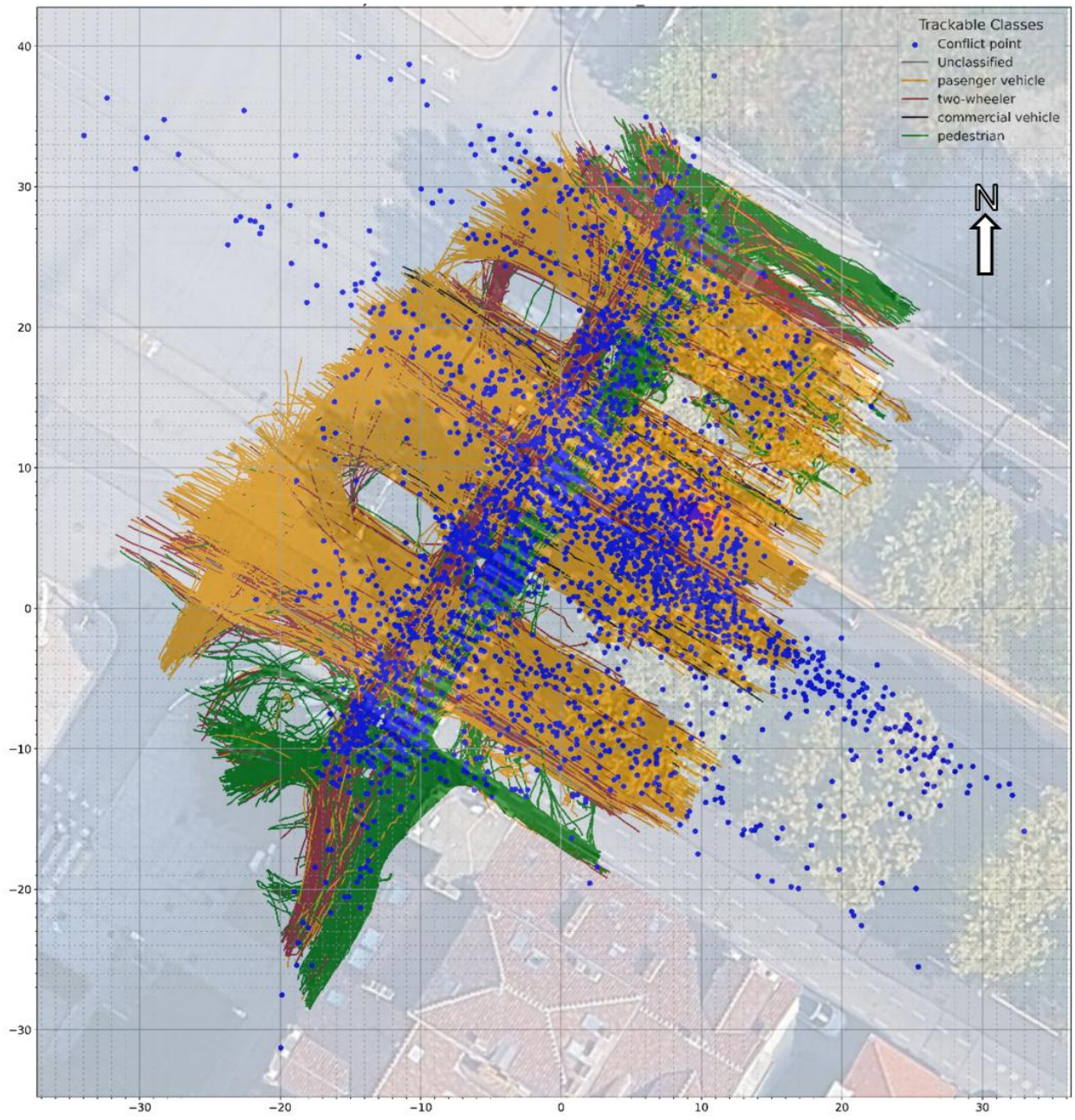

Figure 23 - All trajectory and conflict points, Location 2, Turin

Figure 24 and Figure again present all collected trajectory data and the corresponding conflict points, this time differentiating the road user types involved in the conflicts by colour.

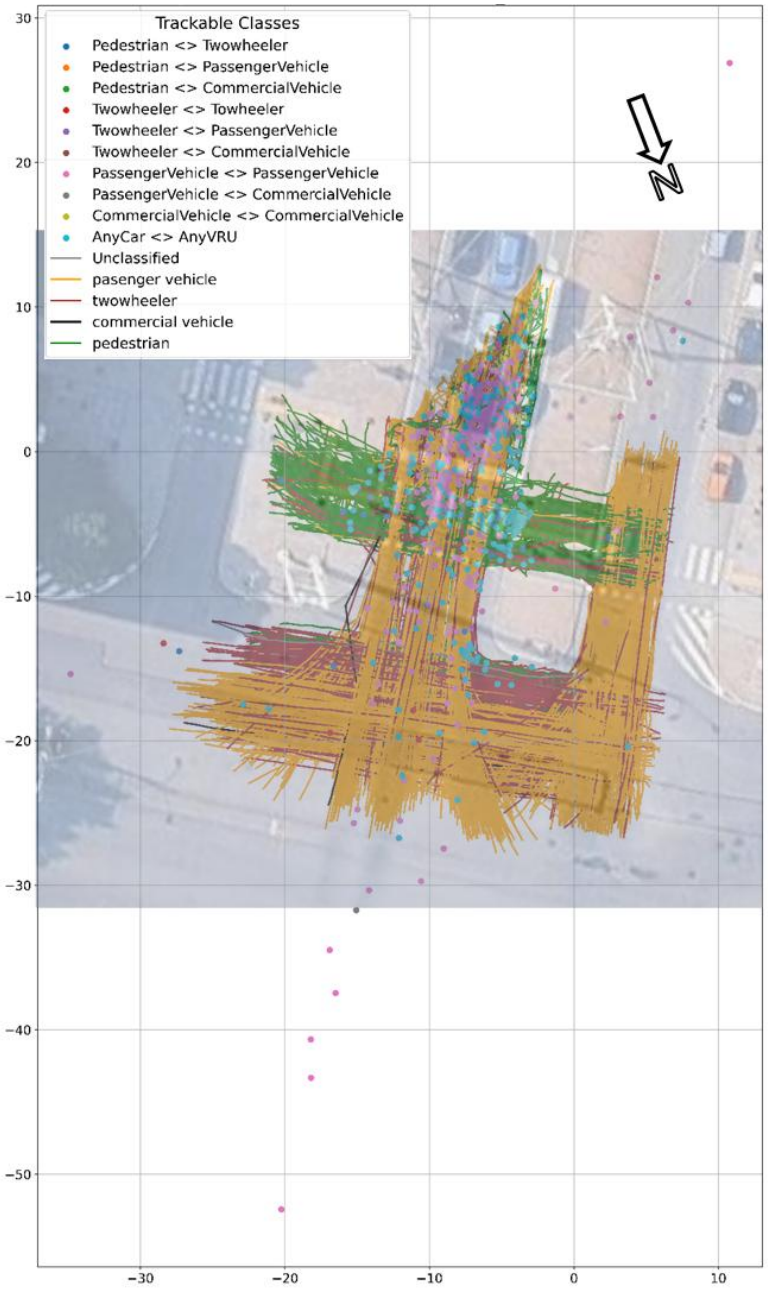

Figure 24 - All trajectory data and conflict points involving different road users, Location1, Turin

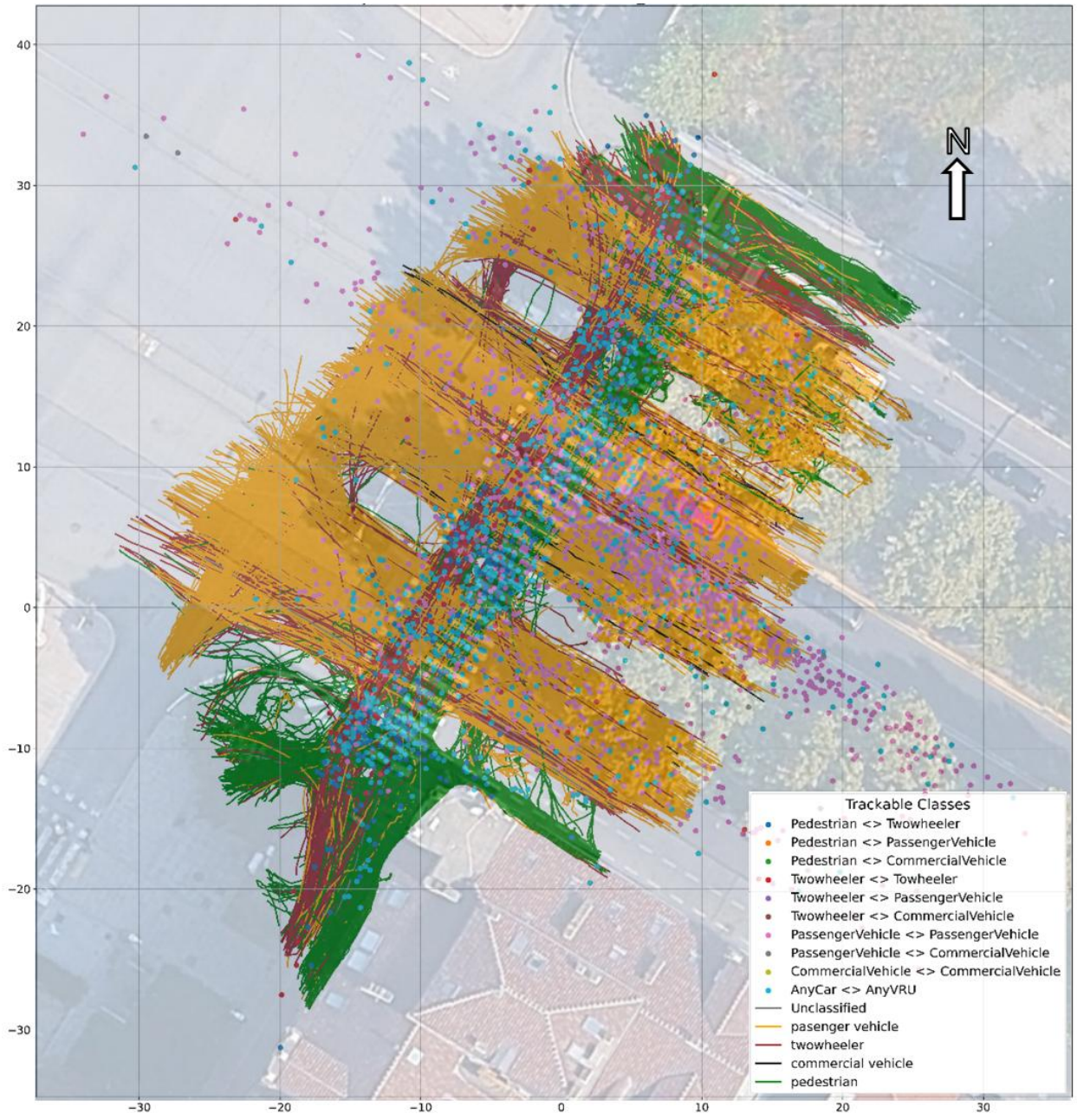

Figure 25 - All trajectory data and conflict points involving different road users, Location2, Turin

Figure and Figure 3 present the conflicting points (CPs) detected between vehicles and VRUs at locations 1 and 2, overlaid with their trajectories. The point colors indicate conflict severity based on the exceedance value $(t_c - minimum\ ITTC)$, where the t_c is the time-to-collision threshold, set to 3 seconds for this study. Figure and Figure 4 display the conflicting points categorized according to the conflict angle between the two road users. The angle is measured between the velocity vectors of the two road users at the moment when the minimum ITTC is observed and is represented using different symbols. Conflicts are classified as follows:

Rear-end: angles < 10°

Side-impact: angles between 10° and 170°

Head-on: angles > 170° (up to 180°)

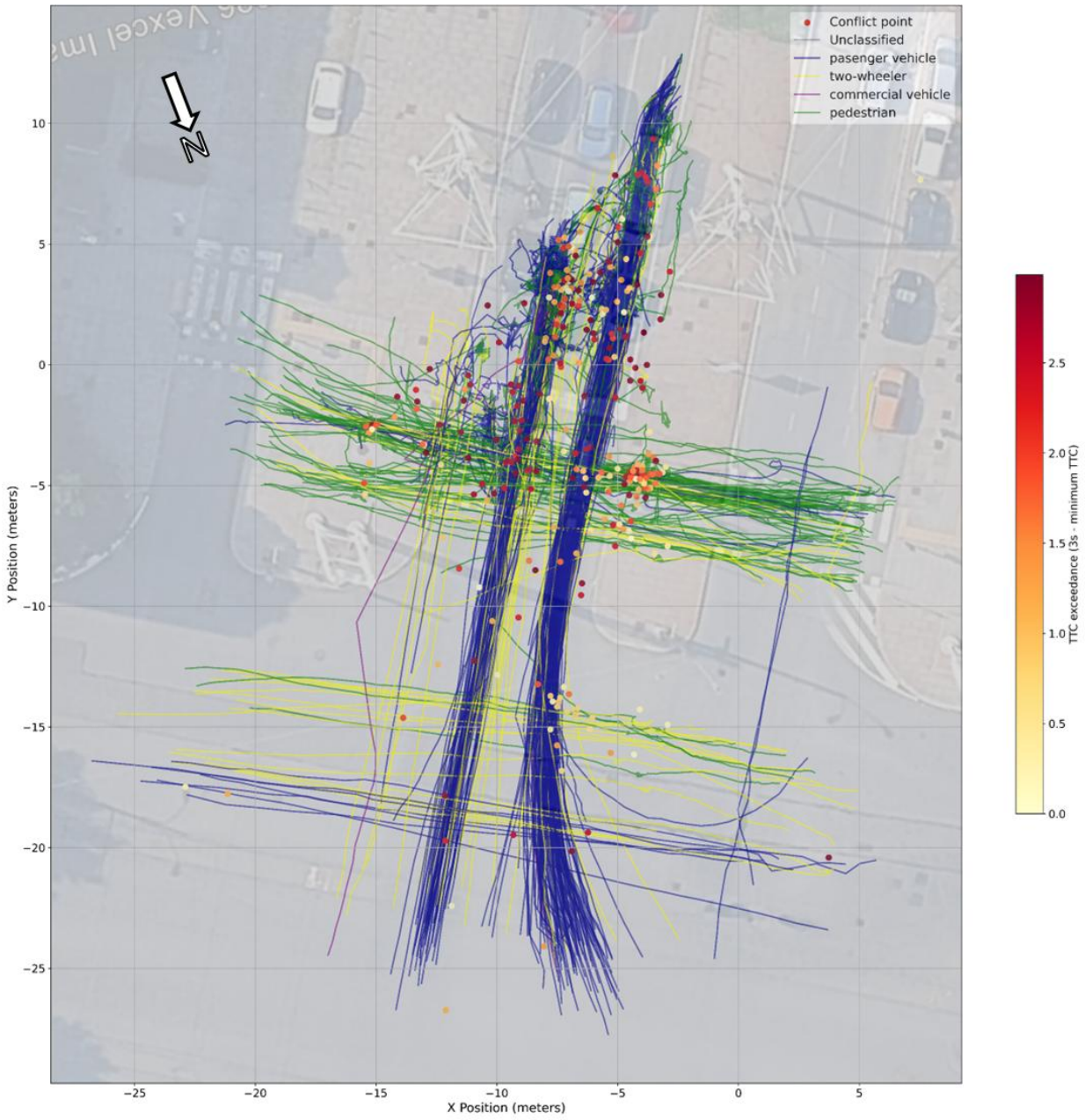

Figure 26 - Trajectory and Conflict points between vehicle and VRU (Location 1)

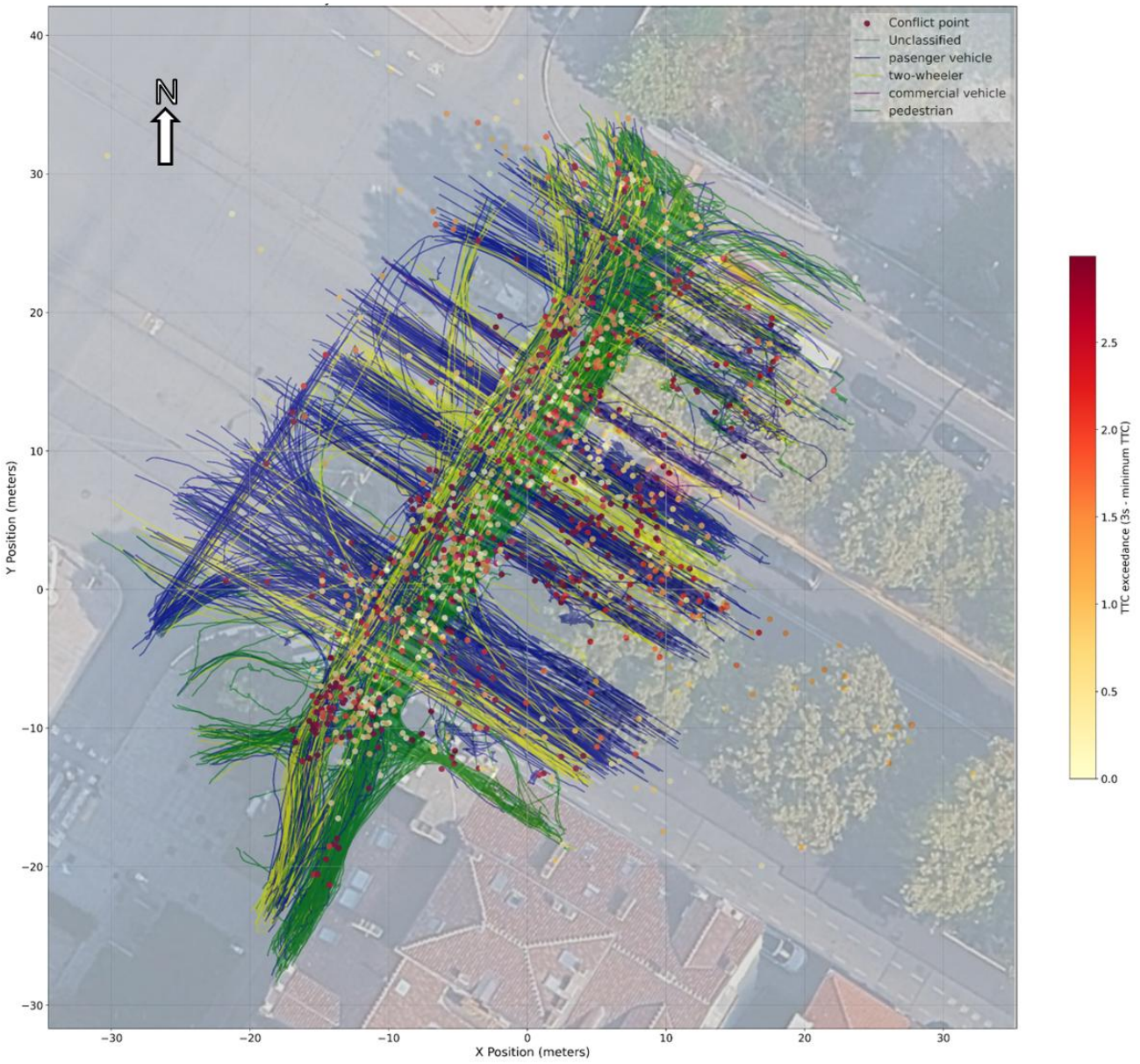

Figure 3 - Trajectory and Conflict points between vehicle and VRU (Location 2)

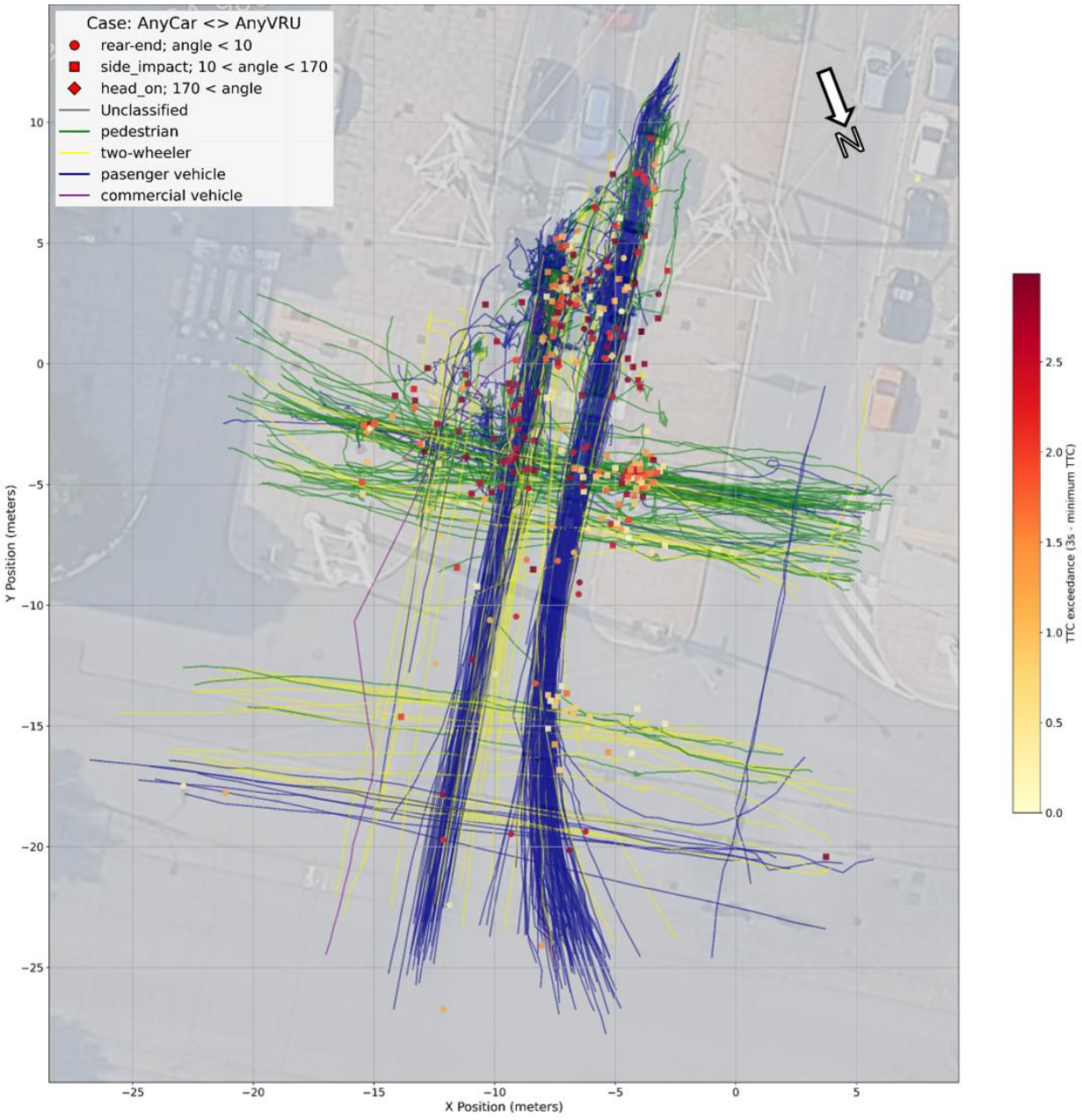

Figure 28 - Trajectory and Conflict points between vehicle and VRU (Location 2)

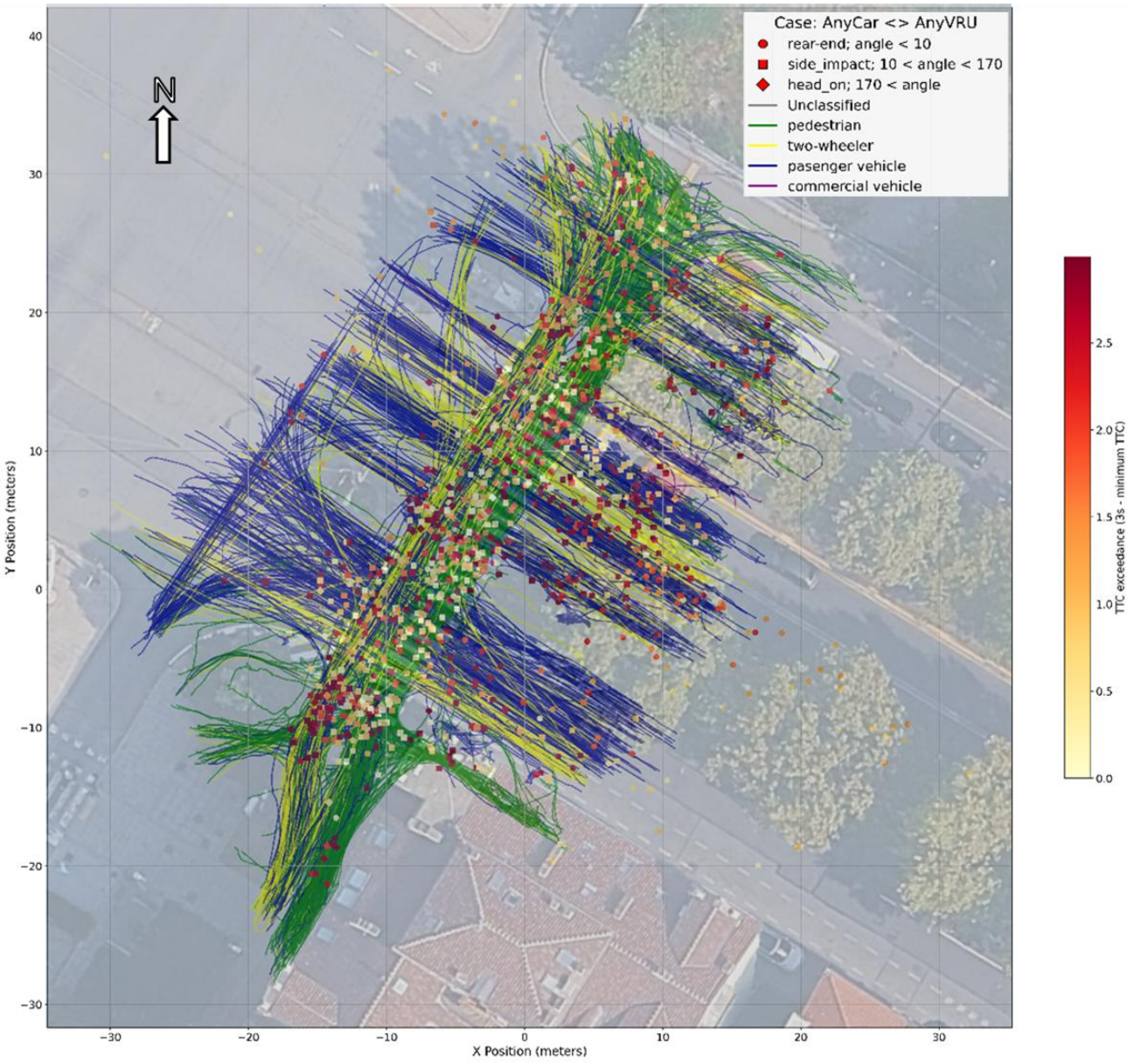

Figure 4 - Vehicle–VRU interaction dynamics, trajectories, and CPs, Location 2, Turin

Figure and Figure show the corresponding hotspots derived from the kernel density estimation (KDE) of the CPs:

a) A weighted KDE, with weights proportional to conflict severity (exceedance).

b) An unweighted KDE based only on frequency.

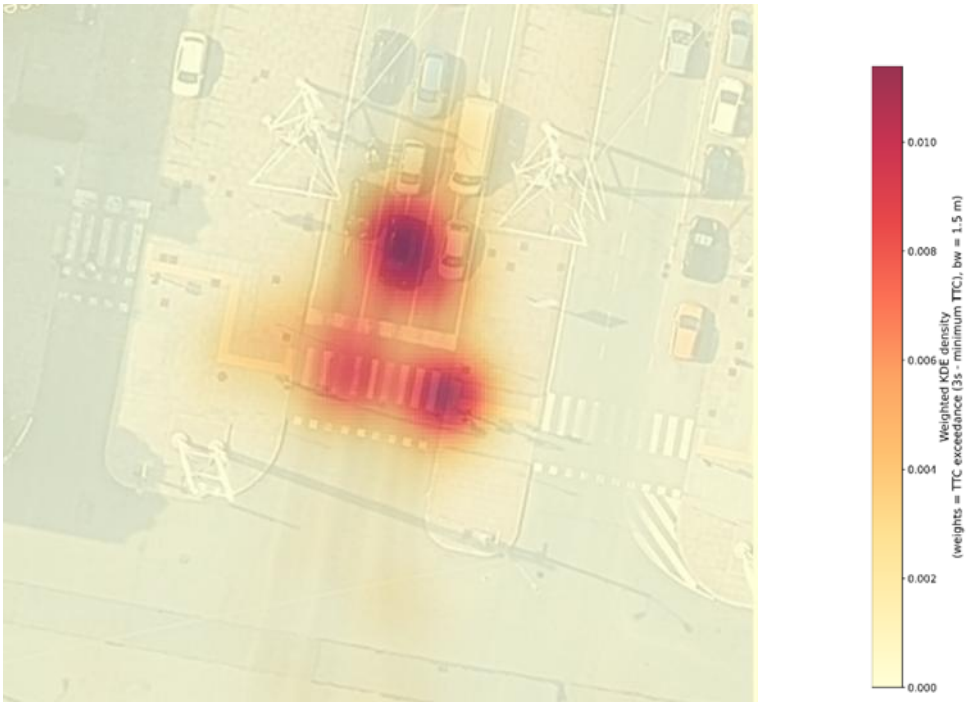

a. Weighted KDE

b. Unweighted KDE

Figure 30 - Conflict points hotspots, Location 1, Turin

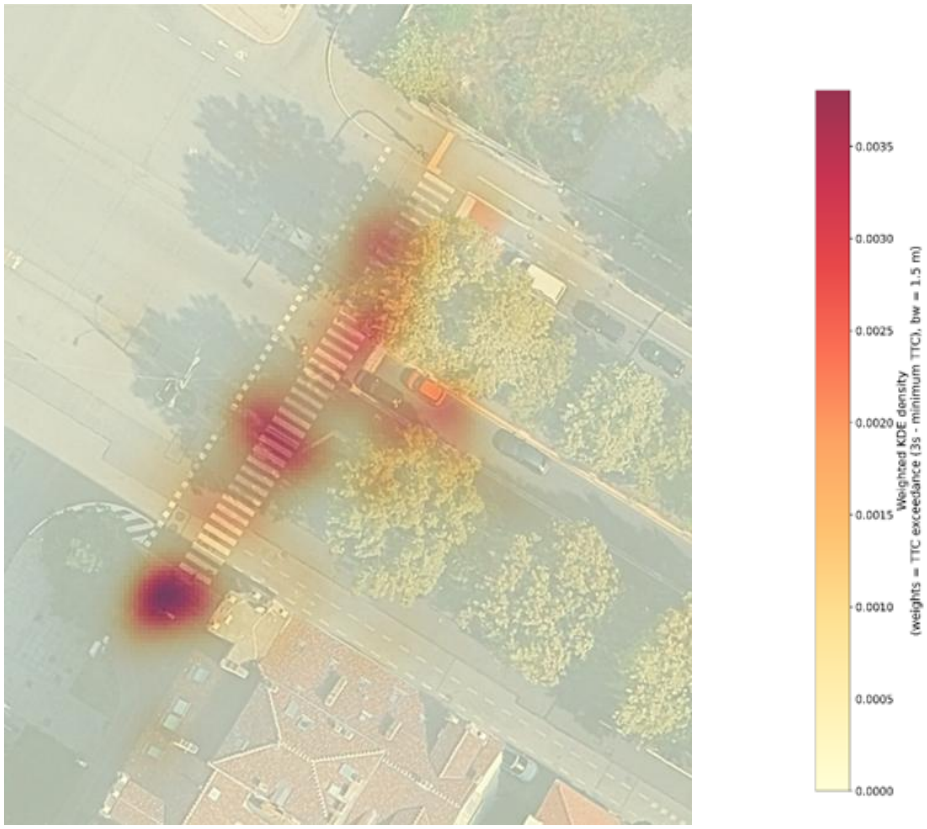

a. Weighted KDE

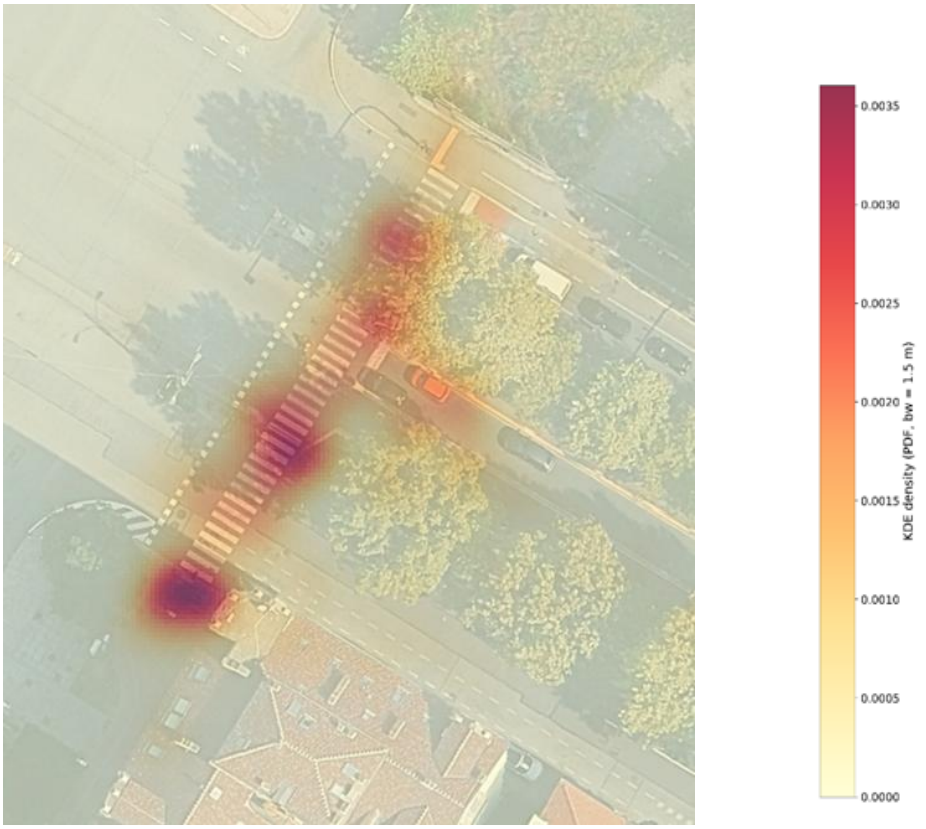

b. Unweighted KDE

Figure 31 - Conflict points hotspots, Location 2, Turin

5 Case Study 3: Padua

Case Study 3 was conducted at the four-legged intersection of Via Gattamelata and Via Gustavo Modena in Padova (Figure 32). About 2.5 hours of data were collected at different times of the day (morning, afternoon, and night) to examine temporal variability (see Table 2). In this case study, data covering the entire intersection was collected during each session.

Figure 5 - Via Gattamelata – Via Gustavo Modena Intersection, Padova

Table 2 - Time and duration of the data collection sessions (Padova)

Record number	Starting Time	Duration (minutes)
Rec 1	10:09	4
Rec 2	10:18	21
Rec 3	13:59	15
Rec 4	14:26	15
Rec 5	15:03	15
Rec 6	15:25	15
Rec 7	15:42	15
Rec 8	22:10	16
Rec 9	22:32	17

The following figures present the results obtained for the Padova case study. Similar to the results shown for the previous case study, Figure displays all recorded trajectories together with conflict points. Figure shows the collected trajectory data and the corresponding conflict points, differentiating the road user types involved in the conflicts. Figure presents the CPs detected between vehicles and vulnerable road users (VRUs), overlaid with their corresponding trajectories. Figure displays the conflicting points involving VRUs categorized according to the conflict angle between the two road users. Figure shows the corresponding hotspots derived from the kernel density estimation (KDE) of the CPs: (a) weighted and (b) unweighted.

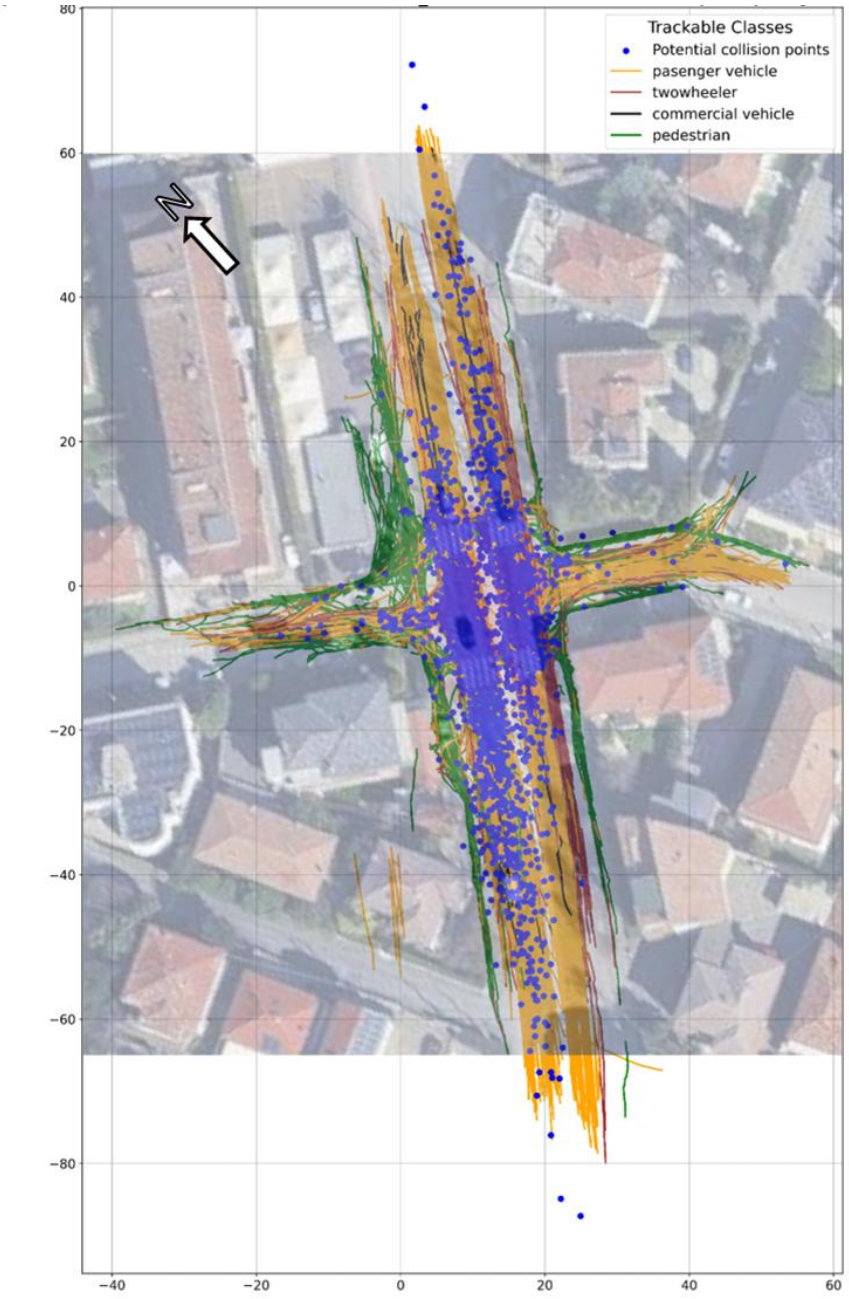

Figure 33 - All trajectory and conflict points, Padova

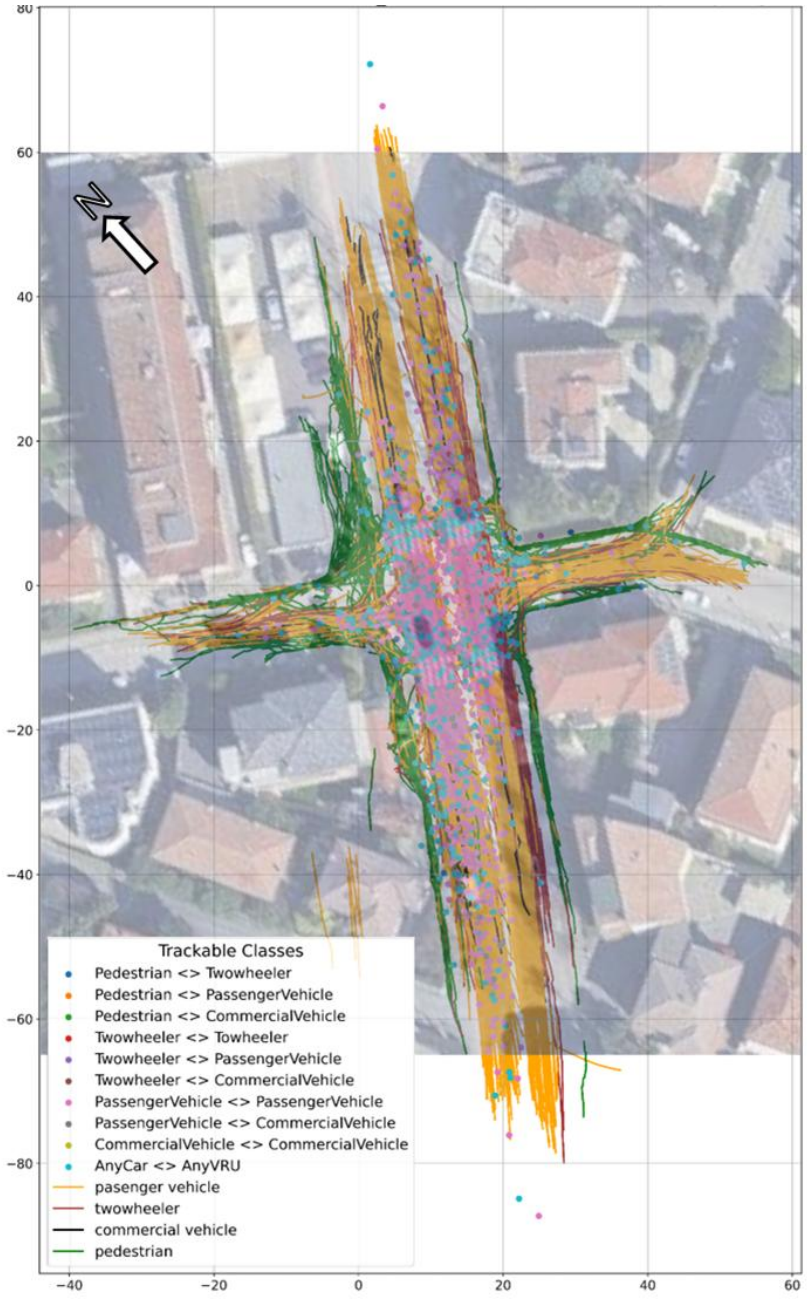

Figure 34 - All trajectory data and conflict points involving different road users, Padova

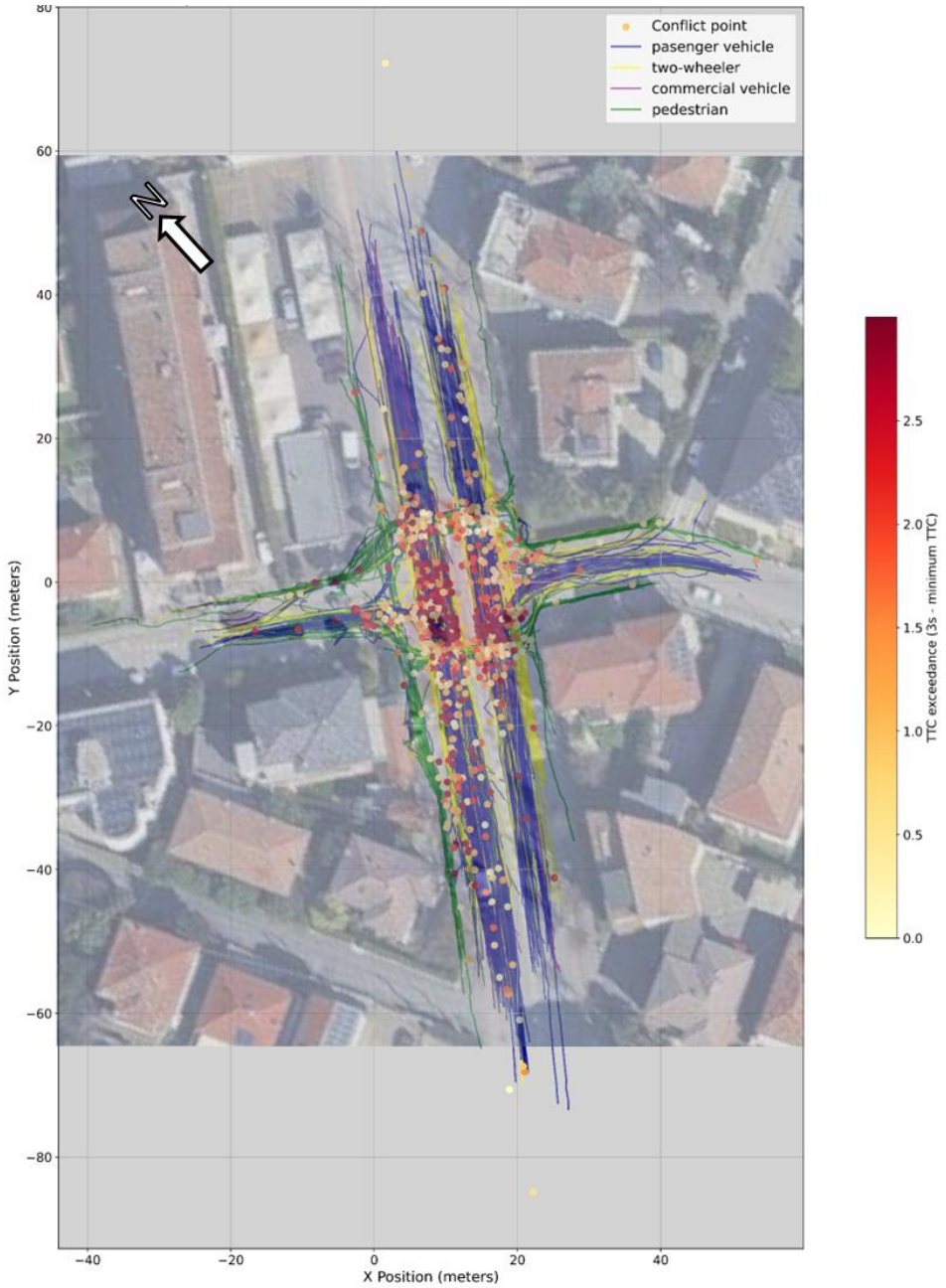

Figure 35 - Trajectory and Conflict points between vehicle and VRU, Padova

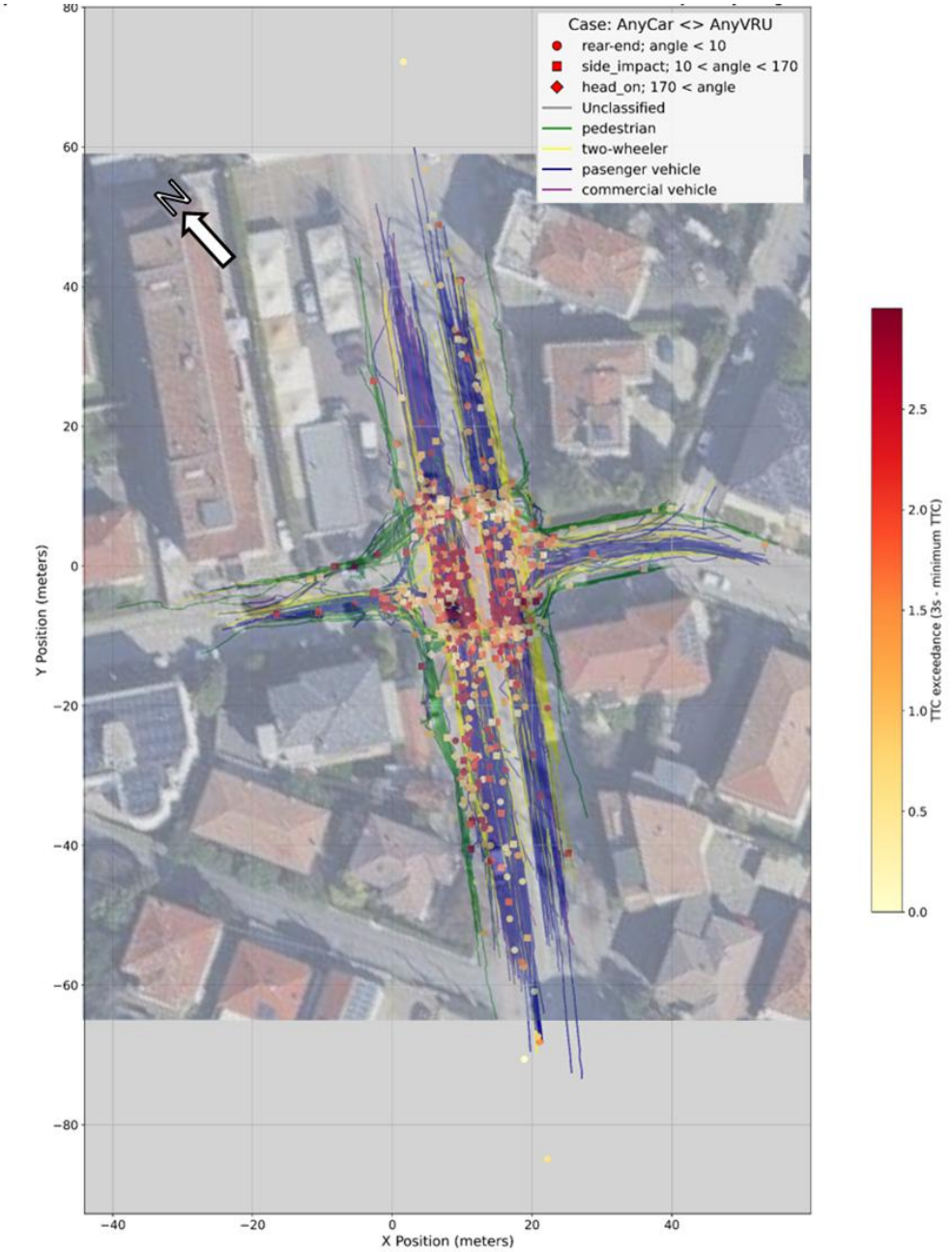

Figure 36 - Vehicle–VRU interaction dynamics, trajectories, and CPs, Padova

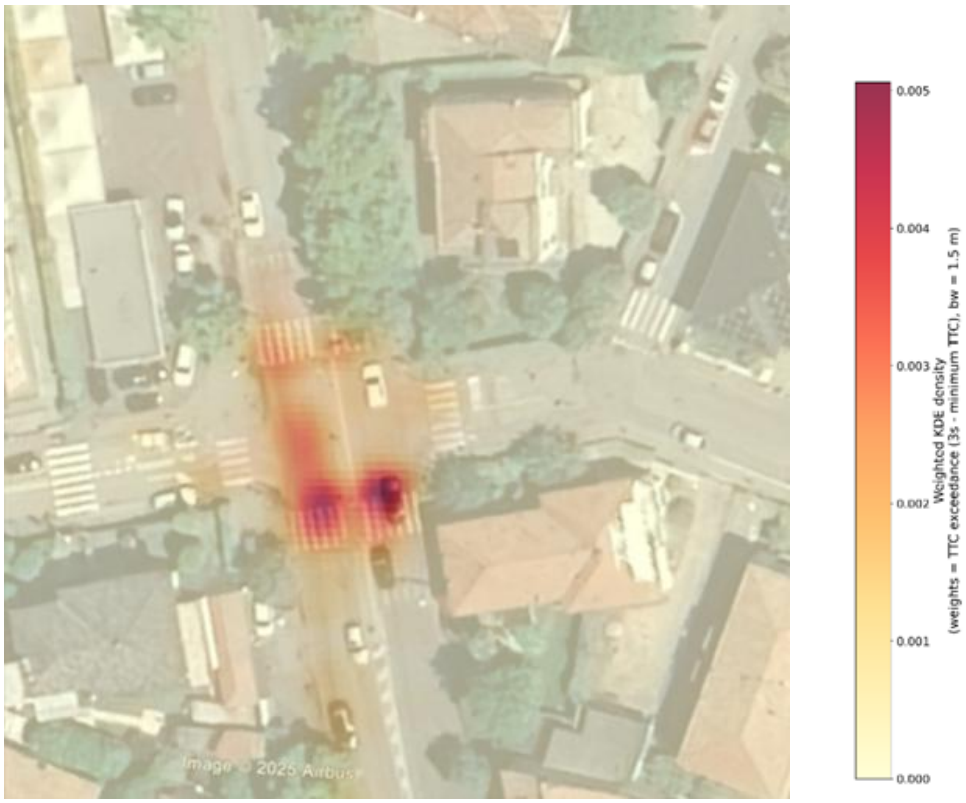

a. Weighted KDE

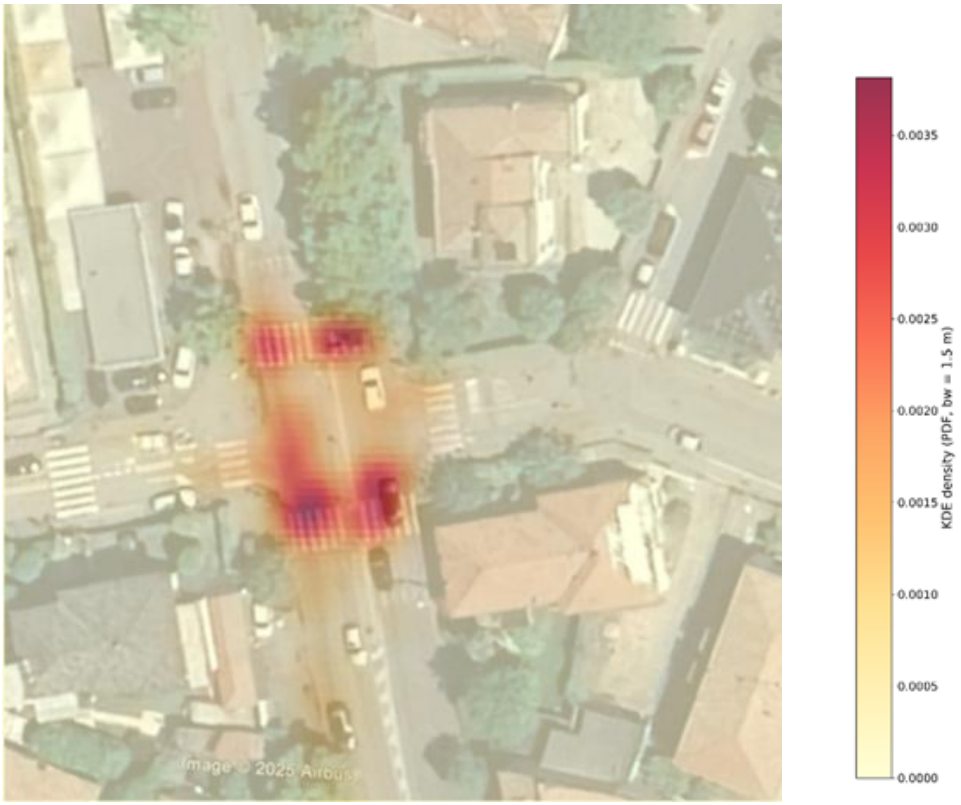

b. Unweighted KDE

Figure 37 - Conflict points hotspots, Padova

References

1. Archer, 2005: Archer, J. (2005). Indicators for Traffic Safety Assessment and Prediction and Their Application in Micro-simulation Modelling: A Study of Urban and Suburban Intersections. Doctoral Dissertation, Royal Institute of Technology (KTH), Stockholm.
2. Bataineh et al., 2023: Bataineh, A., Wu, Y., Fu, C., Li, K. (2023). Evaluating Driving Behavior and Intersection Safety Using Roadside LiDAR. Journal of Transportation Safety & Security.
3. Bella et al. 2021: Bella, F., Silvestri, M. (2021). Vehicle–pedestrian interactions into and outside of crosswalks: Effects of driver assistance systems. TRANSPORT, 36(2), 98-109.
4. FHWA, 2009: Nota: Nel testo citi "FHWA, 2009", ma nella bibliografia fornita l'unica voce corrispondente è del 2008. Ti riporto quella presente: FHWA – Federal Highway Administration (2008). Surrogate Safety Assessment Model (SSAM) – Software User Manual. Report No. FHWA-HRT-08-050, Turner-Fairbank Highway Research Center, McLean, VA.
5. Hydén, 1987: Hydén, C. (1987). The Development of a Method for Traffic Safety Evaluation: The Swedish Traffic Conflicts Technique. Doctoral Dissertation, Lund University.
6. Miller, 1971: Miller, A.J. (1971). Gap Acceptance Theory and Models. Transportation Research, 5(1), 1–14
7. Ni et al., 2016: Ni, Y., Wang, M., Sun, J., and Li, K., “Evaluation of pedestrian safety at intersections: A theoretical framework based on pedestrian-vehicle interaction patterns,” Accident Analysis and Prevention, 96, 118–129 (2016).
8. Svensson, 1998: Svensson, Å. (1998). A Method for Analysing the Traffic Process in a Safety Perspective. Doctoral Dissertation, Lund Institute of Technology.
9. Troutbeck, 1992: Troutbeck, R.J. (1992). Estimating the Critical Gap at Unsignalized Intersections: The Method of Successive Gaps. Transportation Research Part B, 26(4), 253–266.
10. Vennarucci et al., 2025: Vennarucci, A., Manalo, J.R.D., Gagliardi, V., Calvi, A., Bella, F. (2025). Real-Time LiDAR Applications for Assessing the Safety of Vulnerable Road Users at Urban Intersections. In Proceedings of SPIE - The International Society for Optical Engineering. Karsten Schulz, Ulrich Michel, Konstantinos G. Nikolakopoulos, Valerio Gagliardi, Ana Claudia Moreira Teodoro.
11. Zhang et al., 2020: Zhang, H., Anis, M., Li, S., Lord, D., Zhou, Y. (2020). An Improved Vehicle–Pedestrian Near-Crash Identification Method with a Roadside LiDAR Sensor. Journal of Safety Research, 73, 211–224.
12. Tarko, A. (2019). *Measuring Road Safety Using Surrogate Events.* Elsevier. doi:10.1016/C2016-0-00255-